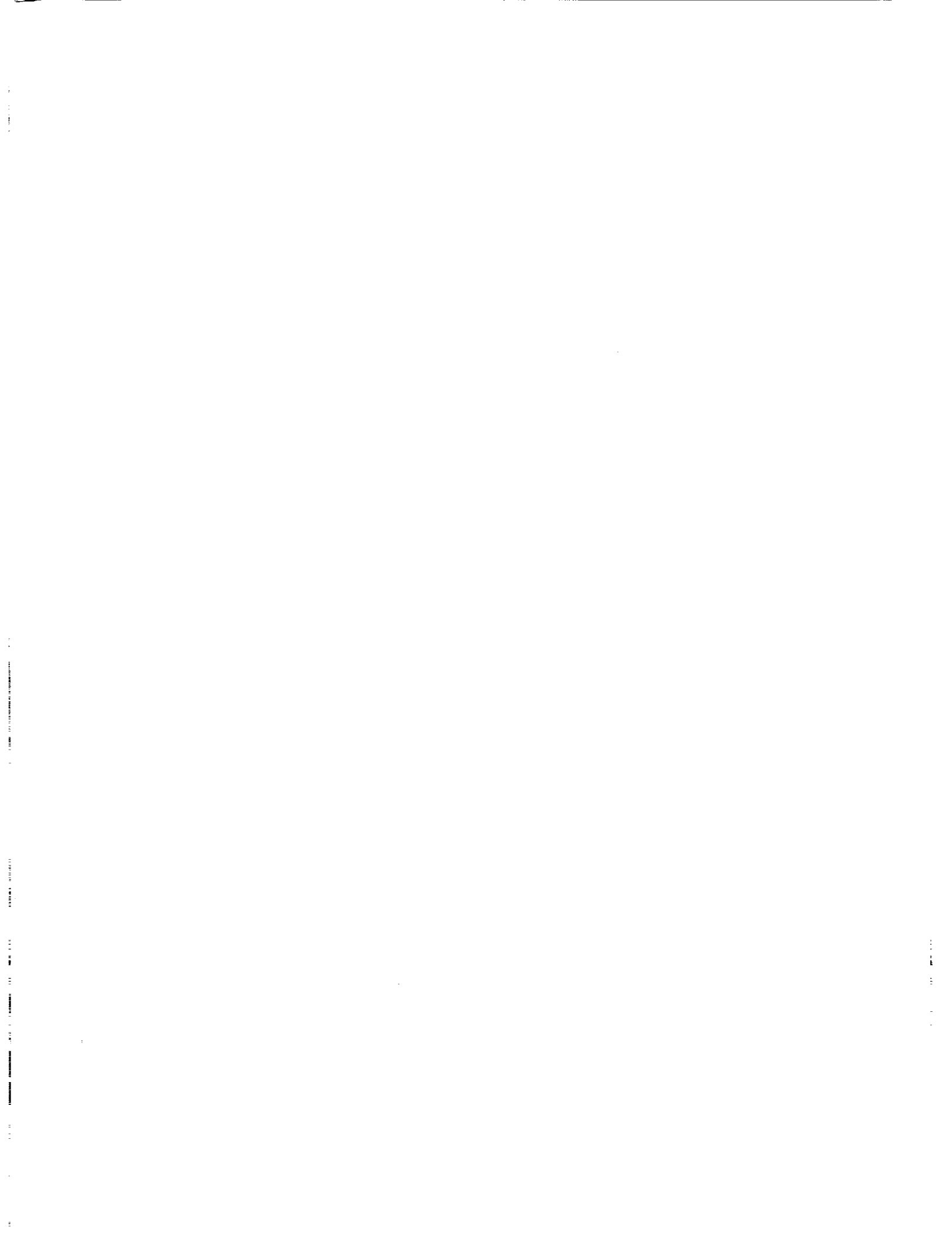


**Scientific Applications**  
**and**  
**Measurements Requirements**



N94-15553

## LASER TRACKING FOR VERTICAL CONTROL

Peter Dunn and Mark Torrence, Hughes STX Corp., Lanham, MD  
Erricos Pavlis, Univ. of Maryland, College Park, MD  
Ron Kolenkiewicz and David Smith, GSFC LTP, Greenbelt, MD

### ABSTRACT

The Global Laser Tracking Network has provided LAGEOS ranging data of high accuracy since the first MERIT campaign in late 1983 and we can now resolve centimeter-level three dimensional positions of participating observatories at monthly intervals. In this analysis, the station height estimates have been considered separately from the horizontal components, and can be determined by the strongest stations with a formal standard error of 2 mm. using eight years of continuous observations. The rate of change in the vertical can be resolved to a few mm./year, which is at the expected level of several geophysical effects. In comparing the behavior of the stations to that predicted by recent models of post-glacial rebound, we find no correlation in this very small effect. Particular attention must be applied to data and survey quality control when measuring the vertical component, and the survey observations are critical components of the geodynamic results. Seasonal patterns are observed in the heights of most stations, and the possibility of secular motion at the level of several millimeters per year cannot be excluded. Any such motion must be considered in the interpretation of horizontal inter-site measurements, and can help to identify mechanisms which can cause variations which occur linearly with time, seasonally or abruptly.

### INTRODUCTION

LAGEOS laser ranging measurements have added significantly to our knowledge of horizontal motion at the observing stations and have helped to improve models of tectonic processes and regional deformation at plate boundaries (Frey and Bosworth, 1988). The tectonic movements are as large as 17 cm/year between fast moving stations such as Huahine and Easter Island which lie astride the Pacific/Nacza plate boundary. The SLR data have demonstrated their ability to measure centimeter per year motions to a few mm/year, but geodesic lengths have usually been used in this work because they directly provide horizontal rates and are independent of vertical variations. The time grain of the horizontal measurements has progressed from annual values (Christodoulidis et al., 1985) to quarterly averages (Smith et al., 1990) as the network has grown and observation and force models have improved.

Accurate vertical control can assist the horizontal positioning in monitoring tectonic processes and the detection of pre- or post-seismic events. Accurate height determination also allows the measurement of post-glacial rebound and the investigation of atmospheric pressure loading at the stations. The scale of an Earth-centered reference system can be defined in a network of SLR stations to establish a global vertical datum. The systems can also be employed to calibrate altimeter instruments by determining the radial component of the orbit of the altimeter mission.

Degnan(1985) has described the various technical methods of accurate range measurement which include careful calibration for electronic path delays and atmospheric refraction, as well as accurate surveys of the distance between a system's electro-optical center and a ground bench-mark. Any systematic errors in the original observations will be preserved in the normal points which we employ in our analysis, and will affect the final position estimates for the stations. Characteristics of each instrument's laser transmitter and detection system must be monitored to ensure that the distribution of satellite returns is normally distributed. Any skewness in the range pattern would bias the normal points, and would usually be caused by errors which would delay the detection of the return, yielding normal points with a longer range value than that from a Gaussian distribution, although this system characteristic will vary with the detection scheme. The magnitude of the signature of the satellite retro-reflector array on the range measurement will also depend on the instrument. We have adopted a value of 251 mm. (Fitzmaurice et al.,1977) for the correction for the offset between the satellite's center-of-mass and its reflecting surface, which would be expected from the multiple photon, leading edge detection MOBLAS systems. Lower power transmitters with alternative detection methods may require corrections differing by a few millimeters.

Errors in station time-keeping can degrade the resolution of the horizontal component of station position, although modern systems using GPS time transfer for epoch time are synchronized to the microsecond, which is an insignificant error at the level of positioning accuracy currently dominated by errors in the satellite perturbation model. Systematic errors in the round-trip time measurement for range are more difficult to control. They will tend to cancel out in the horizontal position measurements of stations with adequate sky coverage, but will directly affect their height estimates. In this treatment we have restricted our analysis to the best calibrated observatories in the network, and have subjected their observations to particularly strict quality control standards. The locations of these stations are shown on the world map of Figure 1, and their positions listed in Table 1, with particular emphasis on the vertical component. The observations from these strong stations now allow us to reduce the interval for determination of 3-dimensional positions from a quarter of a year to a month, and thus provide improved resolution of the rate of any station movement.

#### DATA ANALYSIS METHOD

In our analysis, each SLR measurement constrains the solution of a numerically integrated satellite trajectory. A system of equations which satisfies all of the range information in a least squares sense is developed (Putney,1990) for orbits independently computed with an accurate perturbation model over time spans of approximately a month. The resulting linear system is subsequently solved to yield monthly three-dimensional coordinates of the tracking station positions, together with other geodetic parameters estimated at various time intervals. The motion of the satellite is computed in a reference frame which includes the effect of general relativity about the Earth with an adopted value of  $398600.4415 \text{ km}^3/\text{sec}^2$  for GM, the product of mass and gravitational constant (Ries et al.,1992). The GEM-T3 geopotential model (Lerch et al.,1992) with expanded ocean tides to include significant LAGEOS perturbations was supplemented by third body perturbations from the sun and the moon, together with the planets Mercury through Neptune.

The effects of thermal drag on the satellite were represented by a model of the Earth Yarkovsky effect (Rubincam,1990) with an initial satellite spin axis orientation of 22 degrees,

decreasing by 50% every 6 years. To satisfy remaining unmodelled orbit effects, a secular along-track acceleration was adjusted every 15 days, as well as the phase and amplitude of an along-track component acting once per revolution of the orbit. This once per revolution adjustment parameter is related to the eccentricity excitation vector described by Yoder et al.(1983) and has been found to accommodate variations in the behavior of LAGEOS which have not yet been adequately described (cf. Eanes et al.,1991). The values of secular along-track acceleration determined by the full network over the experimental period is shown in Figure 2. This is a well-determined parameter with a formal uncertainty of about .1 picometer/sec<sup>2</sup>, and the regularly repeating patterns in the early part of the signature have been modelled by several workers (Anselmo et al.,1983; Afonso et al.,1989; Scharoo et al.,1991) using theories based on both Earth-reflected and direct solar heating. The unusual behavior of the along-track signature commencing in 1990 is not very well predicted by these models.

Figure 3 shows the orthogonal components of the once-per revolution acceleration estimates, which are more weakly determined than the direct effect, and have formal errors of about the same size as a typical value. The cosine function of orbital angle from equator crossing measures unmodelled perturbations in the equatorial plane, particularly those associated with solar position and radiation pressure. The unusual variation in it's amplitude indicates a change in the satellite's behavior in 1989 and again in 1991, and recent observations have shown that the irregular behavior continues in 1992. Bertotti and Iess (1991) have suggested that torques on the spacecraft due to eddy currents and gravity gradient would lead to chaotic spin dynamics in 1991 or 1992, and this could help explain these results. The once per revolution perturbations affect monthly orbital fits to the ranging observations by as much as ten centimeters, but when modelled according to the values of Figure 3, the root mean square fit of each month's data remains below five centimeters, and with this precision it is possible to resolve the vertical components of the selected stations at the centimeter level each month.

Ocean loading at appropriate locations was applied (IERS Standards: McCarthy, 1991), although this semi-diurnal effect would be very small when averaged over the monthly position estimates of stations with adequate sky coverage, but would have an effect on stations which track at favored times of the day (or night). Earth rotation and orientation parameters (EOP) were taken from a global solution in which they were adjusted daily in the J2000 reference system with the effects of dynamic polar motion included, and in which the UT1 time published by the International Earth Rotation Service was fixed for one day of each month to establish a longitude frame. In the global solution the station position for each site was estimated, but its motion was modelled according to Smith et al.(1990), resulting in a consistent reference frame throughout the eight year experimental period. In both the global solution for EOP and the monthly analysis which yielded the height values presented here, the stations' reference system was set by fixing the horizontal position components of Greenbelt (latitude and longitudes) and Maui (latitude). The results for monthly values of station height are reported only if coverage for both of the fiducial stations at Greenbelt and Maui reached a minimum of nine LAGEOS passes, and if there were adequate data from each individual station. A nutation series according to Wahr(1981) was adopted and the effect of solid Earth tides at the stations was also computed according to Wahr(1981)

#### LASER DATA QUALITY CONTROL

Each of the observatories whose vertical motion was monitored in this analysis contains a well calibrated system that has been in operation since late 1983. During the lifetime of each

station, continuous improvements are made to the system through up-grades in hardware and software. Any disturbance at an instrument is monitored with accurate resurveys of the system's eccentricity (optical center with respect to an associated ground marker) as well as of any change in the surveyed distance of the calibration tower used for system delay correction. The eccentricity offsets for the various MOBILAS instruments fielded by the Goddard Space Flight Center are listed in Table 2. They have been retrieved from the Crustal Dynamics Data Information System (CDDIS) in December 1991 and their correctness will directly affect the estimated heights given in Table 1, as well as any measure of vertical motion. The remaining observatories in the network were assumed stationary during the eight year period and their positions refer to the optical axis of each telescope, which is the estimated parameter in our data reduction. Any improved information on eccentricity surveys can be used to efficiently up-date the marker positions, and it is not necessary to repeat the full data reduction process. On the other hand, techniques for direct estimation of station velocity will require accurate eccentricity values at the outset of the analysis to connect the positions of each occupation at a site.

Information concerning calibration characteristics of each system is accessible through the CDDIS, although it has already been used in the processing of the raw range measurements and is thus embedded in the normal points. As corrections to the calibration procedures are uncovered by subsequent analysis, it is necessary to compensate for any effects that retro-active improvements might exert on station position. Subtle engineering problems in the detection system must be remedied in a pre-processing stage using the original time-of-flight observations, but many of the data corrections can be represented by pass-by-pass or longer term range or timing bias parameters, and the design of our analysis facilitates the incorporation of historical updates using linear shifts based on the partial derivatives of range or clock bias computed in the initial time-consuming computation of normal equations. Several corrections to the released data were required. In particular, range corrections to Arequipa observations were applied: 4 cm to each measurement up to March 1986 to allow for the improved survey of the calibration tower noted in the CDDIS description of this station, as well as another 3 cm until July 1988 at which time improved system delay calibration procedures indicated this offset (Husson, 1988). Range errors of this magnitude would significantly affect any estimates of vertical motion occurring at the rate of a few mm/year, and the possibility of similar anomalies at other locations is closely monitored. The most compelling indication of engineering effects in station position is an abrupt change in station height to a subsequently maintained level: this was clearly seen when earlier, uncorrected Arequipa data was used in quarterly solutions shown in the lower frame of Figure 4. When the height of the station was held fixed at a value estimated over the 13 year data span, the monthly estimates of range bias shown in Figure 4 indicate error in the earlier observations of the correct magnitude.

#### ANALYSIS OF VERTICAL MEASUREMENTS

The independent monthly values of height at the three stations with the lowest month-to-month variation seen in our analysis are given in Figures 5a,b and c. The least significant figures in millimeters of the distance from an average Earth semi-major axis of 6378136.3 m. appear on the vertical scale and the measurements are qualified by error estimates of twice their formal standard deviation based on the final fit of the range observations to each orbital arc. Although the ranges themselves are formally accurate to better than a centimeter, systematic residual signatures of several centimeters in amplitude are observed due to uncompensated errors in force, measurement and Earth orientation models. The effect of atmospheric refraction on the laser ranges is modelled according to Marini and Murray (1973) who assumed a spherically

stratified atmosphere based on surface pressure measurements. Herring (1988) has shown that range corrections due the refractivity formula, the zenith range correction and the elevation dependence of the range correction formula should only be a few millimeters at 20 degree elevation angle, which is the lower limit for most of the systems. However, any long term variations in station barometer accuracy or in the effects of lateral gradients in the atmosphere (see Abshire and Gardner, 1985) will directly affect the vertical estimates. The SLR systems could thus be used to monitor aberrations in the dry component of atmospheric refraction which would not be separable from the wet component in nearby microwave instruments.

The possibility of errors in the adopted eccentricities must also be considered, particularly for stations which have undergone changes of system occupation, such as Greenbelt, Quincy and Huahine (see Table 2). The system changes at the North American sites coincided with collocation tests which cross-calibrated each instrument's ranging machine as well as its eccentricity. The transportable systems are periodically returned to Greenbelt for up-grades and collocation calibration against MOBLAS-7, but do not usually undergo a collocation test at their working location. The Huahine position shows more variation than the other sites but, because TLRs-2 eccentricity errors are minimized by employing a precise repositioning technique, this behavior is more likely to be due to the influence of the early, less accurate MOBLAS-1 measurements .

Considerable deviation from uniform motion can be noted in the height variation for some stations, and most of the estimated height rates shown in Table 3 are not significant compared to their quoted uncertainties, which are twice the formal standard error based on the fit of the individual values to a straight line. The measures of scatter of the height values about the mean listed in Table 1 are only reduced by a millimeter or two when a linear fit is substituted. The height statistic has been used as a quality control factor in earlier work measuring the horizontal component of motion (see, for example Table 3 of Smith et al., 1990). Considering the scatter of a station's height about a mean (or uniformly moving) value as a measure of the 'quality' of the station's performance, we see that it depends as much on system stability and careful calibration as upon the precision of the observations, and the lower values of height scatter at Greenbelt, Yarragadee and Arequipa testify to the reliability of these instruments.

Post-glacial rebound of the Earth from the melting of continental ice sheets starting roughly 18,000 years ago produces changes in the gravity field as it affects the long-term evolution of the LAGEOS orbit and have been reported by Yoder et al. (1983) and Rubincam (1984). Wagner and McAdoo (1986) present a simple uniform viscosity model for the rate of change of radial position due to post-glacial rebound based on the Ice-2 maps of Wu and Peltier(1983), and this model is complete enough to include all the SLR sites. The values of vertical uplift at each observatory predicted by the model have been taken from Figure 5 of Wagner and McAdoo(1986) and are compared in Table 3 with the height rates estimated from the laser data from the SLR stations, arranged for convenience by tectonic plate. Very little correlation can be seen between the modelled and observed values of up-lift, even in Europe, where the 4 mm/year rate expected from the model is within the detection capability of the SLR systems. On the other hand, neither the model nor the SLR observations taken at Greenbelt can confirm sinking of eastern North America as required by tide gauge data (see Trupin 1991) : the absence of higher degree terms due to the lack of a lithosphere in their treatment has been noted by Wagner and McAdoo and could explain the model results. James and Morgan (1990) have shown in more detail how modelling assumptions of the properties of the lithosphere can cause disagreement with sea level observations, and they have also indicated that horizontal motions due to post-glacial rebound in

North America and Fennoscandia can amount to 4 mm/year from plausible models. This movement is predicted in the Hudson Bay region where vertical movement can amount to over 10 mm/year, and both components are clearly within the resolution capability of a modern SLR system occupying this region in an extended campaign.

It is possible that further investigation of the SLR observations will uncover a source of instrument error which would alias into the vertical component of station position. However, the apparent rate of 4 mm/year observed at Arequipa is large enough that no SLR analysis should assume a stationary vertical component and expect accurate baseline measurements to distant stations. Only explicit separation from the vertical component by considering geodesic lengths will allow the definition of accurate horizontal motion.

## CONCLUSIONS

The stability of the radial component of position at the strongest SLR observatories in an eight year time span suggests that vertical motion is bounded by 2 or 3 mm/year and this analysis does not confirm variations suggested by models of post-glacial rebound. Periodic signatures apparent in the height results may represent seasonal variations of a geophysical nature, but do not produce significant long term trends. These accurate estimates of station height can help in the calibration of satellite altimeters as well as to establish scale for positioning techniques which degrade as a function of distance on a global scale, such as GPS campaigns in close proximity to the SLR Observatories. The data quality control which must be exercised to retain the full scaling accuracy of the laser ranges is not so stringent in the analysis of GPS networks as they benefit from strong orbital geometry when multiple satellites are simultaneously tracked. On the other hand, accurate relative position measurements of each instrument's reception center from a ground marker is critical in both space techniques and must be carefully monitored. The capability with which the Global Laser Tracking Network can control vertical scale will grow with the increased number of retro-reflector-carrying satellites expected to be in high Earth orbit in the next few years. As observations from LAGEOS 2 are supplemented by concentrated tracking of the currently orbiting ETALON spacecraft, time resolution of any subtle vertical motion should also be improved.



## REFERENCES

- Abshire, J.B. and C.S. Gardner, "Atmospheric Refractivity Corrections in Satellite Laser Ranging", IEEE Trans. on Geosc. and Rem. Sense. GE-23, 1985
- Afonso, G.F., Barlier, M., Carpino, P., Farinella, F., Mignard, M., Milani, A.M., Nobili, A.M., "Orbital Effects of LAGEOS Seasons and Eclipses", Ann. Geophys. A 7(5), 501-514, 1989
- Anselmo, L., Bertotti, B., Farinella, A., Milani, A.M., Nobili, A.M., "Orbital Perturbations due to Radiation Pressure for a Spacecraft of Complex Shape", Celest. Mech. 29, 27, 1983
- Bertotti, B., and L. Iess, "The Rotation of LAGEOS", J. Geophys. Res., 96, 2431-2440, 1991
- Christodoulidis, D.C., D.E. Smith, R. Kolenkiewicz, S.M. Klosko, M.H. Torrence and P.J. Dunn, "Observing Tectonic Plate Motions and Deformations from Satellite Laser Ranging", J. Geophys. Res., 90(B11), 9249-9263, 1985
- Degnan, J.J., "Satellite Laser Ranging: Current Status and Future Prospects", IEEE Trans. on Geosc. and Rem. Sense. GE-23, 1985
- Eanes, R.J. and M.M. Watkins, "Temporal Variability of Earth's Gravitational Field from Satellite Laser Ranging Observations", XX Gen. Ass. IUGG Symp. No. 3, Vienna, 1991
- Fitzmaurice, M.W., P.O. Minott, J.B. Abshire and H.E. Rowe, "Prelaunch Testing of the Laser Geodynamic Satellite (LAGEOS)", NASA Tech. Paper 1062, 1977
- Frey, H.V. and J.M. Bosworth, "Measuring Contemporary Crustal Motions: NASA's Crustal Dynamics Project", Earthqu. and Volc. 20(3), 1988
- Husson, V.S., "First Six Month Data Processing Report", BFEC Report, October 1988
- James, T.S., and W.J. Morgan, "Horizontal Motions due to Post-Glacial Rebound", Geo. R. Lett. 17(7) 1990
- Lerch, F.J., "Geopotential Models of the Earth from Satellite Tracking, Altimeter and Surface Gravity Observations: GEM-T3 and GEM-T3S", NASA TM 104555, 1992
- McCarthy D.D. (ed.), IERS Standards (1989), IERS Tech. Note 3, Central Bureau of IERS, Observatoire de Paris, 1989
- Putney, B., R. Kolenkiewicz, D. Smith, P. Dunn and M.H. Torrence, "Precision Orbit Determination at the NASA Goddard Space Flight Center", Adv. Space Res., 10(3), 197-203, 1990
- Ries, J.C., R.J. Eanes, C.K. Shum and M.M. Watkins, "Progress in the Determination of the Gravitational Coefficient of the Earth", in press, 1992

Rubincam, D.P., "Postglacial Rebound Observed by LAGEOS and the Effective Viscosity of the Lower Mantle", *J. Geophys. Res.*, 89(B2), 1077-1087, 1984

Rubincam D.P., "Drag on the LAGEOS Satellite", *J. Geophys. Res.*, 95, 4881-4886, 1990

Scharoo, R., K.F. Wakker, B.A.C. Ambrosius and R. Noomen, "On the Along-track Acceleration of the LAGEOS Satellite", *J. Geophys. Res.*, 96, 729-740, 1991

Smith, D.E., R. Kolenkiewicz, P.J. Dunn, J.W. Robbins, M.H. Torrence, S.M. Klosko and R.G. Williamson, "Tectonic Motion and Deformation from Satellite Laser Ranging to LAGEOS", *J. Geophys. Res.*, 95(B13), 22013-22041, 1990

Trupin A.S., "The Effect of Global Change and Long Period Tides on the Earth's Rotation and Gravitational Potential", U. Col. Ph.D. Thesis, 1991

Wagner, C.A. and McAdoo, D.C., "Time Variation in the Earth's Gravity Field Detectable With GRM Intersatellite Tracking", *J. Geophys. Res.* 91(B8), July, 1986

Wahr, J.M., "The Forced Nutations of an Ellipsoidal Rotating, Elastic and Oceanless Earth", *Geophys. J. R. Astron. Soc.* 64, 1981

Wu, P., and Peltier, W.P., "Glacial Isostatic Adjustment and the Free Air Gravity Anomaly as a Constraint on Deep Mantle Viscosity", *Geophys. J. R. Astron. Soc.* 74, 1983

Yoder, C.F., J.G. Williams, J.O. Dickey, B.E. Schutz, R.J. Eanes and B.D. Tapley, "Secular Variation of Earth's Gravitational  $J_2$  Coefficient from LAGEOS and Non-tidal Acceleration of Earth Rotation", *Nature* 303, 1983

TABLE 1 : STATION POSITIONS

		LATITUDE	LONGITUDE	HEIGHT	ST.ERR.	ST.DEV	NO.
		DEG MNSEC	DEG MNSEC	METERS	MILLIMETERS		MONTHS
GREENBELT	7105	39 1 14	283 10 20	19.931	2	16	69
QUINCY	7109	39 58 30	239 3 19	1107.119	2	18	67
MON.PEAK	7110	32 53 30	243 34 39	1839.746	2	20	73
YARAGADEE	7090	-29 2 47	115 20 48	242.080	2	16	69
HUAHINE	7123	-16 44 1	208 57 32	46.110	5	23	22
AREQUIPA	7907	-16 27 57	288 30 25	2492.945	2	17	52
MATERA	7939	40 38 56	16 42 17	536.551	2	19	60
WETZEL	7834	49 8 42	12 52 41	661.842	4	24	45
GRAZ	7839	47 4 2	15 29 36	540.125	3	20	55
RGO	7840	50 52 3	20 10	76.114	3	21	69
SIMOSATO	7838	33 34 40	135 56 13	100.175	4	25	51

TABLE 2 : ECCENTRICITY OFFSETS

			START	STOP	N(mm)E(mm) UP(mm)		
GREENBELT	7105	MOBLAS-7	84 1 1	84 3 22	16	-26	3169
			84 3 22	85 7 29	17	-32	3169
			85 7 29	89 10 12	17	-31	3168
			89 10 12	90 7 25	35	-40	3162
			90 7 25	91 12 31	-14	-33	3153
	7918	TLRS-4	90 4 6	90 7 23	-7	-5	2613
QUINCY	7109	MOBLAS-8	84 1 1	86 9 18	-29	11	3124
			86 9 26	91 3 17	-27	12	3138
		TLRS-4	91 3 19	91 8 19	-5	0	2651
		MOBLAS-8	91 11 18	91 12 11	-19	5	3184
		91 12 12	91 12 31	-35	-3	3184	
MON.PEAK	7110	MOBLAS-4	84 1 1	88 4 30	-33	-15	3210
			88 4 30	91 12 31	-33	-16	3213
YARAGADEE	7090	MOBLAS-5	84 1 1	87 8 13	3	11	3185
			87 8 13	91 12 31	3	10	3177
HUAHINE	7121	MOBLAS-1	84 1 1	86 3 13	8	1	3662
			87 7 14	87 10 8	0	0	1453
	7123	TLRS-2	88 3 16	88 9 1	0	0	1437
			89 4 24	89 9 3	0	0	1482
			90 3 15	90 8 20	-1	3	1459
			91 4 5	91 9 4	-2	4	1482
GROUND MARKER DISTANCES							
		X(mm)	Y(mm)	Z(mm)			
	7105 TO 7918	-14419	5137	9457			
	7121 TO 7123	1458	807	501			

TABLE 3 : COMPARISON WITH POST-GLACIAL REBOUND MODEL

TECTONIC PLATE	STATION	MODEL	OBSERVED	
N. AMERICAN	GREENBELT	3	1.7	+/-2 mm/year
	QUINCY	3	1.5	2
PACIFIC	MON.PEAK	1	2.6	2
	HUAHINE	1	3.2	4
AFRICAN	MATERA	1	2.3	2
EURASIAN	WETZEL	4	-1.5	3
	GRAZ	4	.9	2
	RGO	4	-.2	2
AUSTRO-INDIAN	YARAGADEE	1	1.4	2
S. AMERICAN	AREQUIPA	-2	4.1	2
UNKNOWN	SIMOSATO	-3	2.2	4

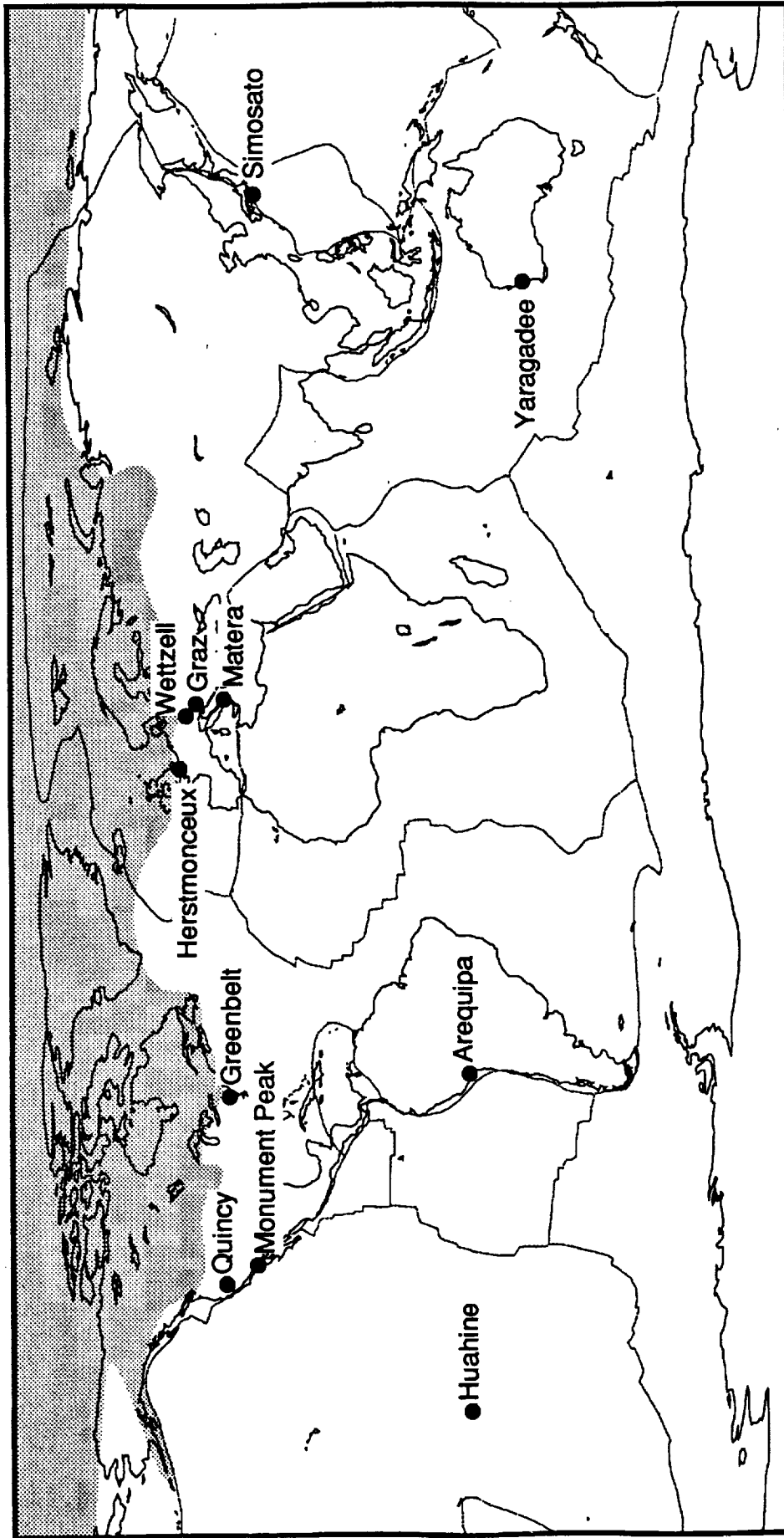


Figure 1 : A world map showing the selected stations and Tectonic and Ice Sheet Boundaries.

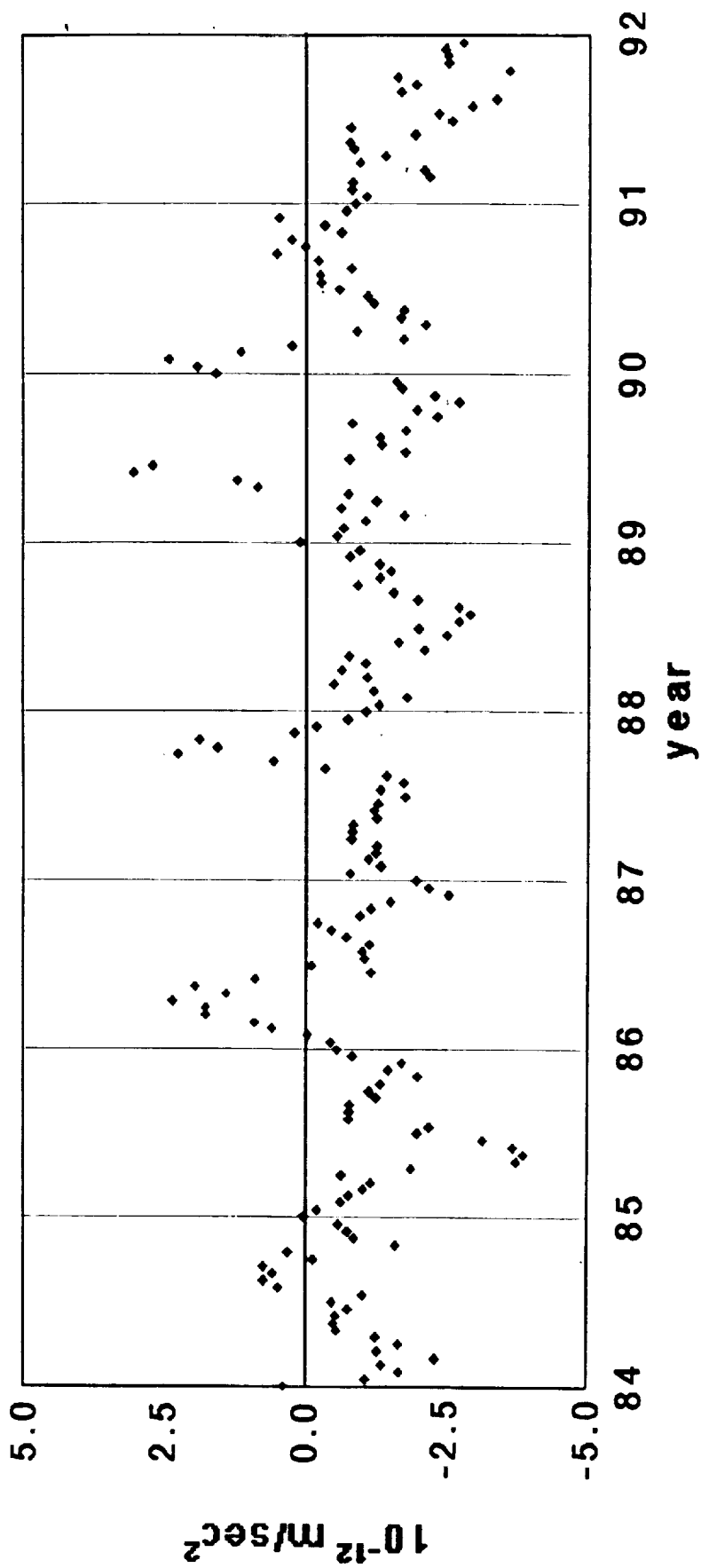


Figure 2 : Semi-monthly values of direct estimates of along-track accelerations.

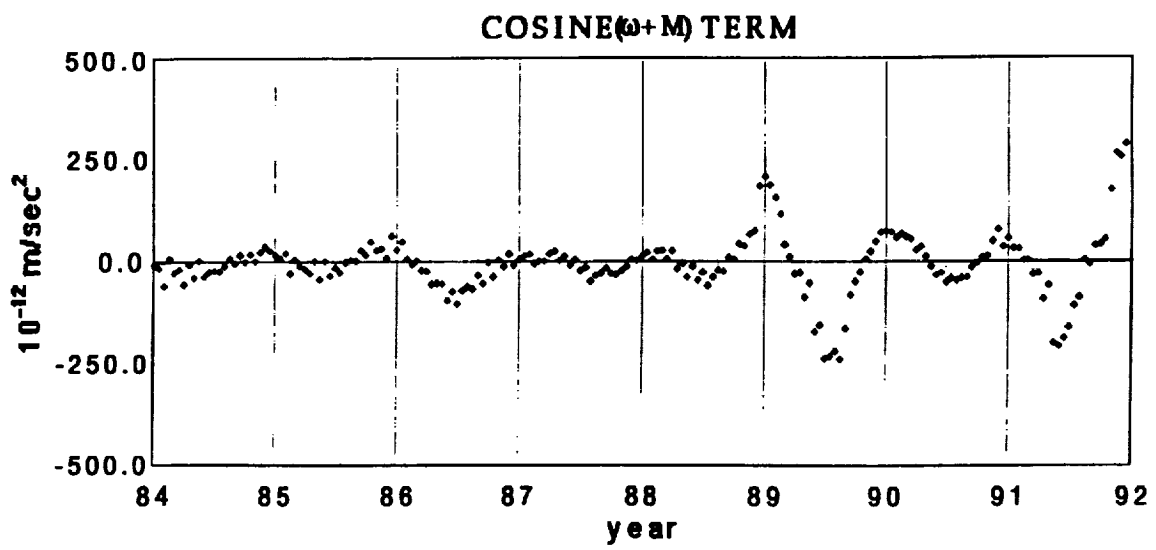
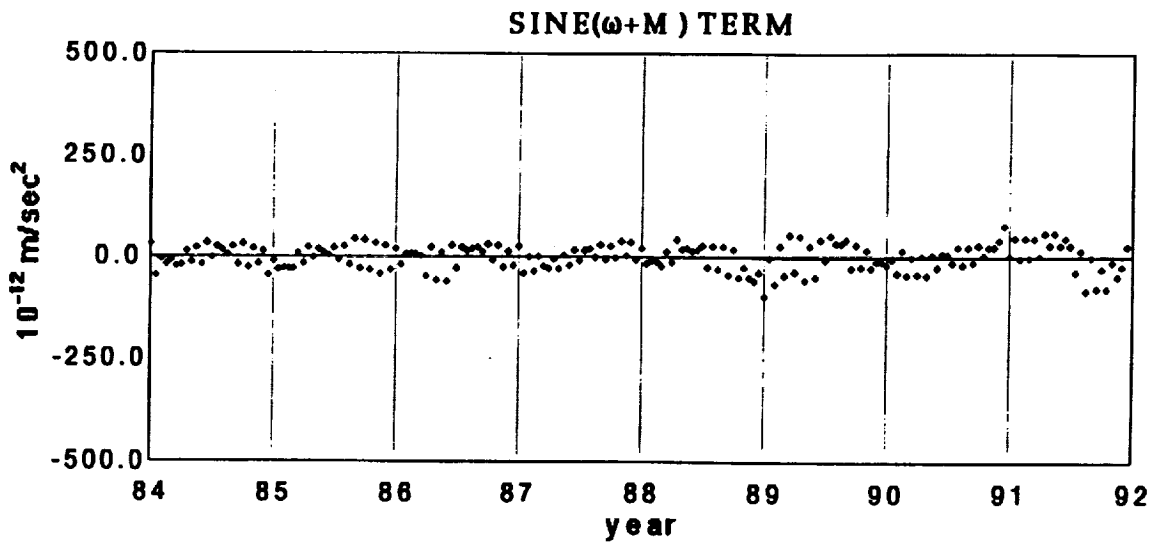


Figure 3 : Semi-monthly values of the once-per revolution acceleration



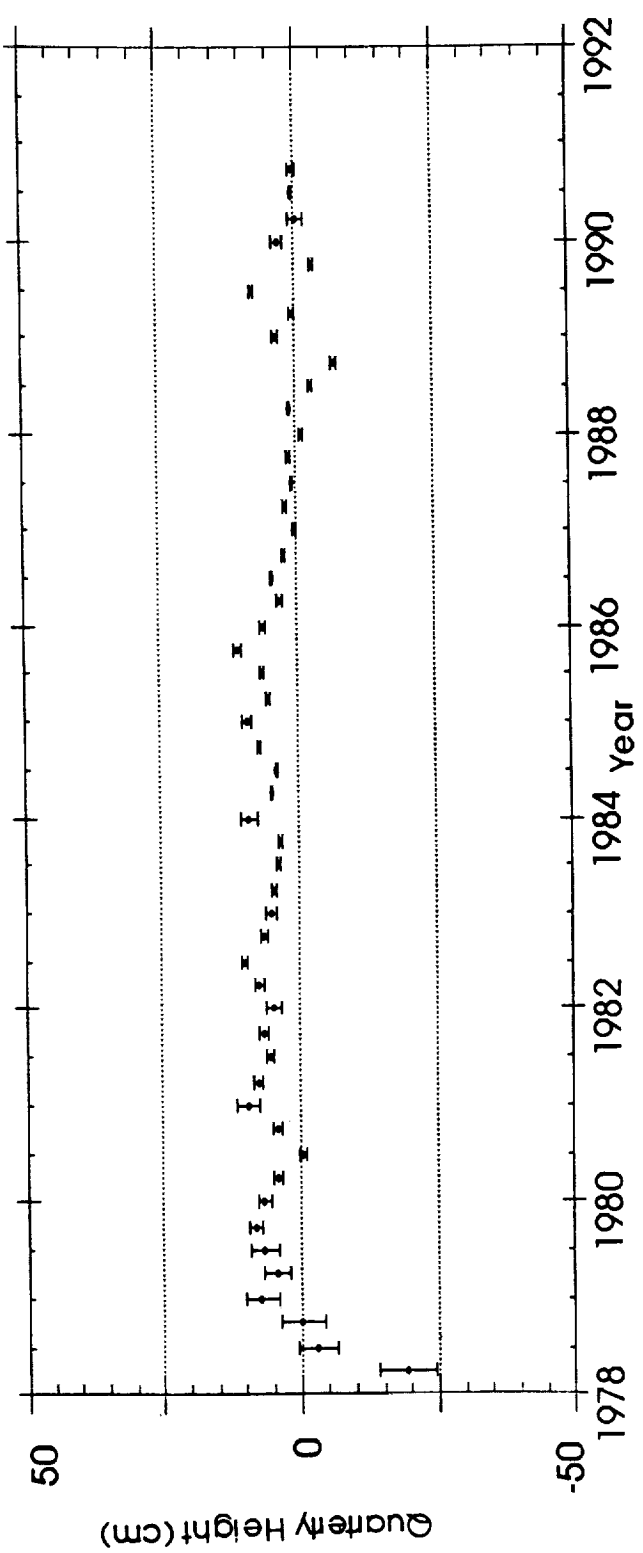
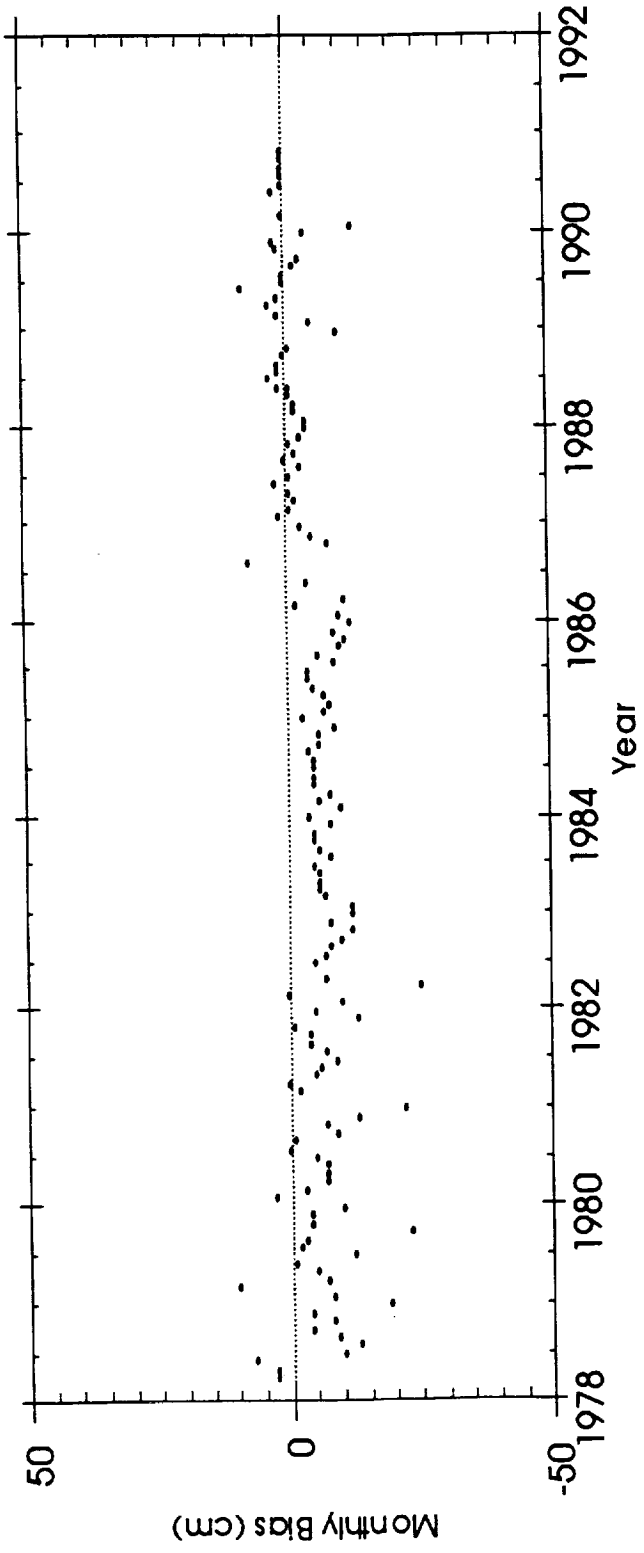


Figure 4 : Arequipa Range Bias Estimates and Equivalent Station Height Variations

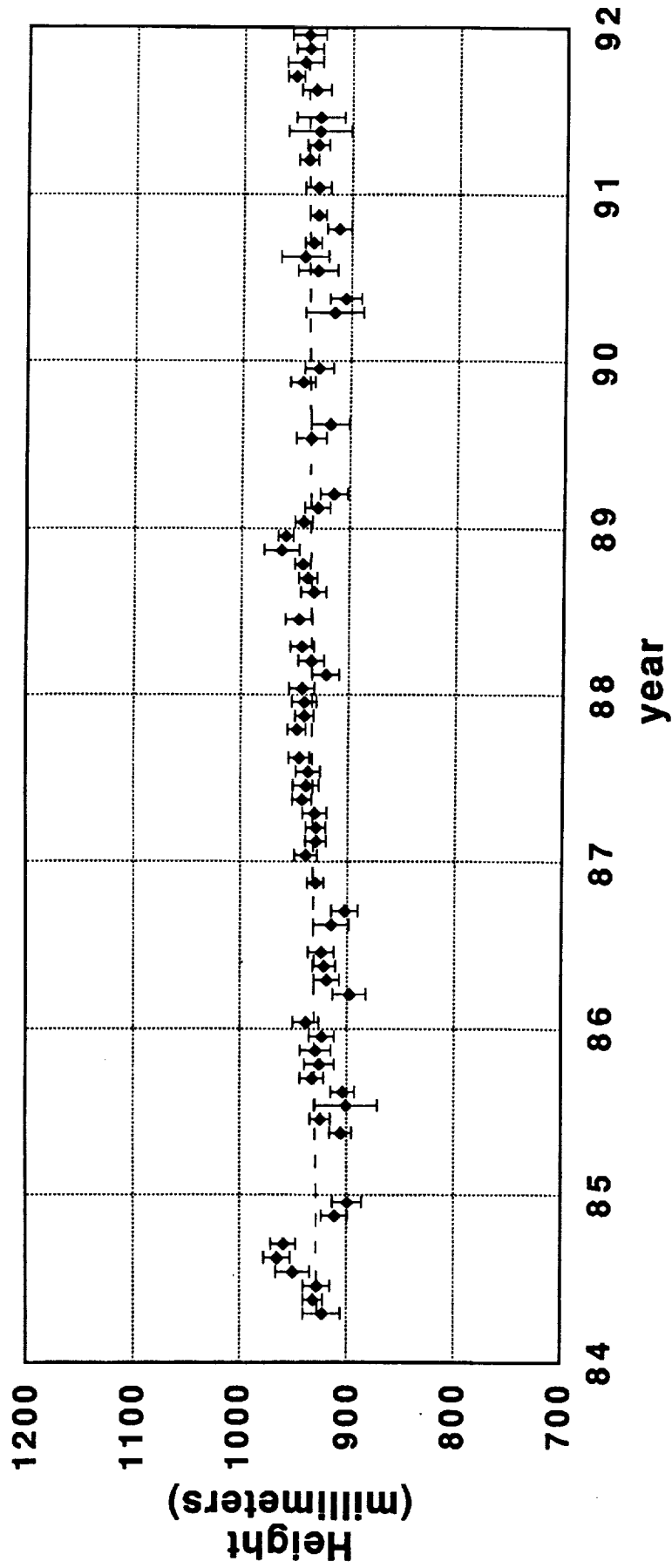


Figure 5a : Monthly estimates of the height of Greenbelt

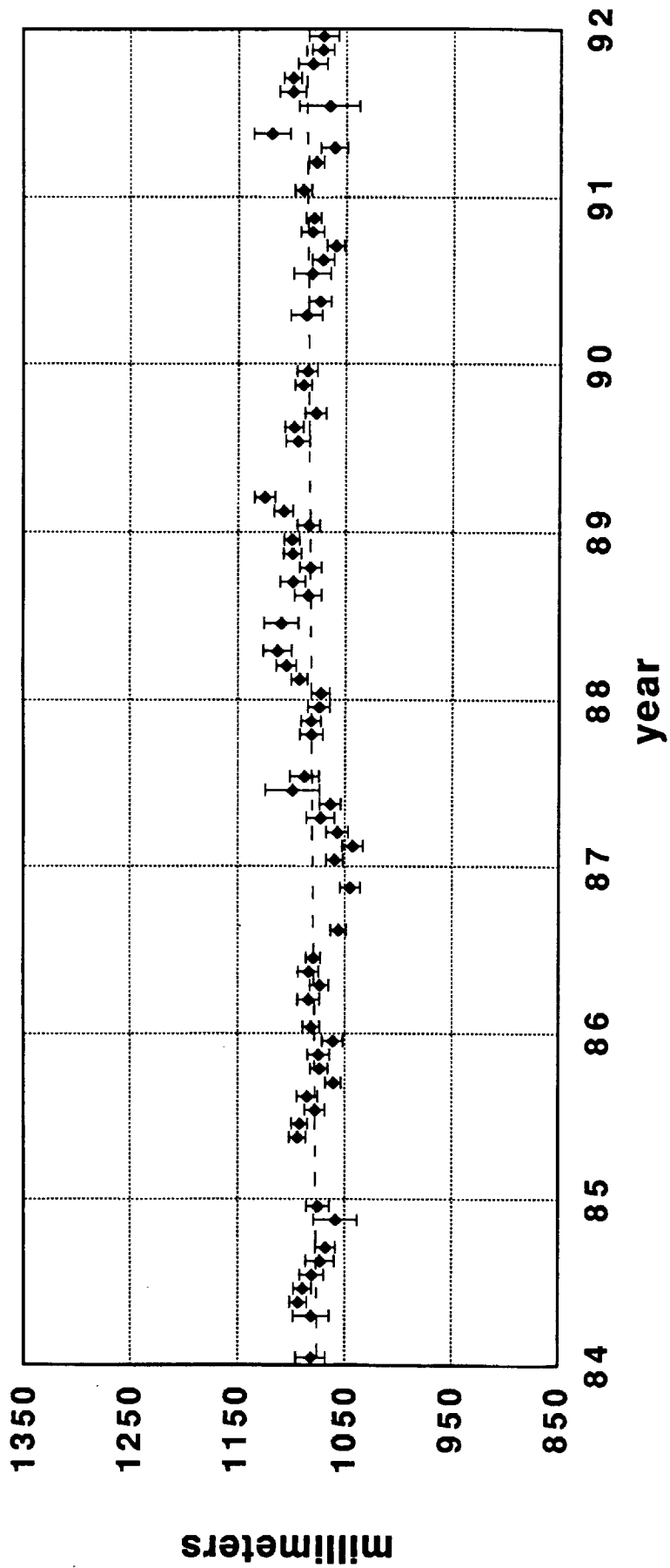


Figure 5b : Monthly estimates of the height of Yarragadce

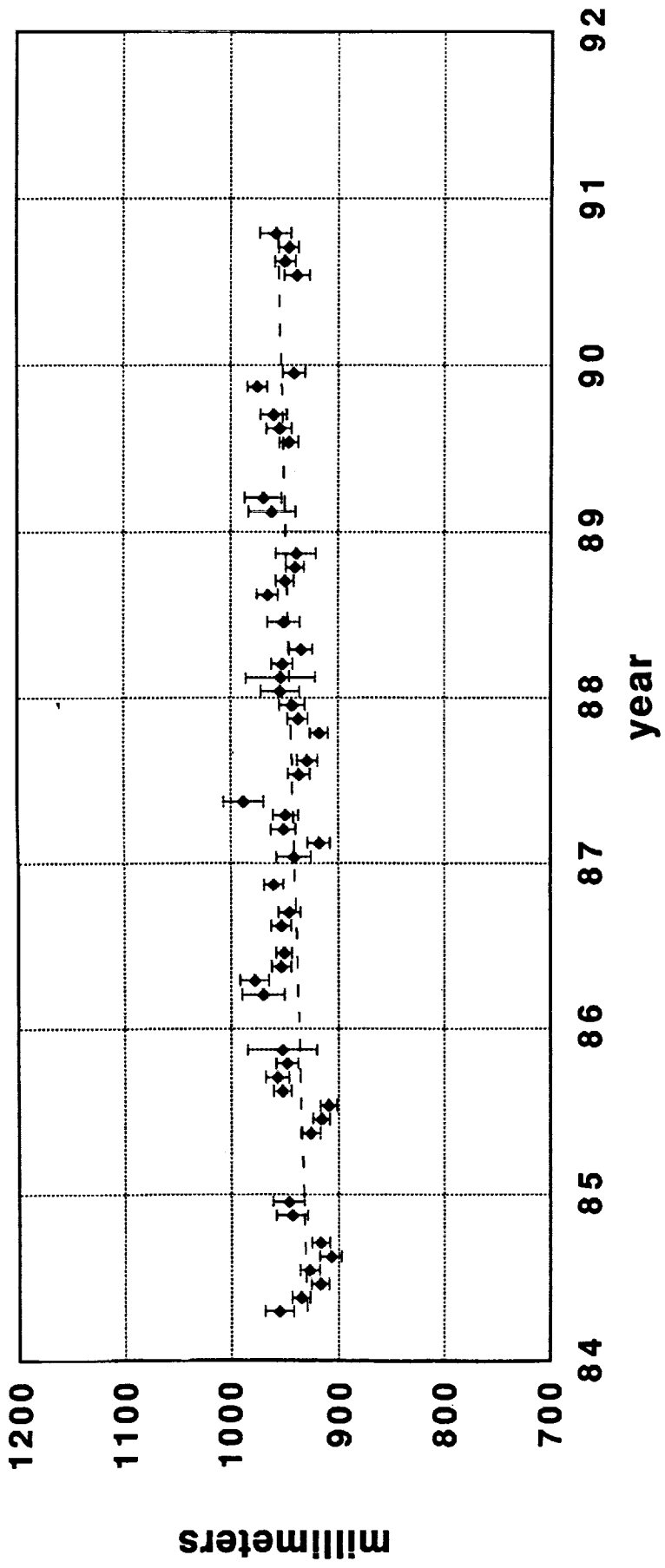


Figure 5c : Monthly Estimates of the height of Arcquipa

## Laser Ranging Network Performance and Routine Orbit Determination at D-PAF

F.-H. Massmann, Ch. Reigber, H. Li, R. König,  
J.C. Raimondo, C. Rajasenan, M. Vei

Deutsches Geodätisches Forschungsinstitut (DGFI), Abt. I, and  
German Processing and Archiving Facility (D-PAF)  
Münchner Str. 20  
D-8031 Oberpfaffenhofen  
Germany

### Summary

ERS-1 is now about 8 months in orbit and has been tracked by the global laser network from the very beginning of the mission. The German processing and archiving facility for ERS-1 (D-PAF) is coordinating and supporting the network and performing the different routine orbit determination tasks.

This paper presents details about the global network status, the communication to D-PAF and the tracking data and orbit processing system at D-PAF. The quality of the preliminary and precise orbits are shown and some problem areas are identified.

### 1. Background

On July 17, 1991, the first European (ESA) Remote Sensing Satellite (ERS-1) was successfully launched from Kourou, French Guayana. The satellite is equipped with a number of active microwave instruments for the monitoring of the Earth's environment (see figure 1). In order to make full use of the measurements the ERS-1 orbit has to be known very precisely. For this purpose ERS-1 is carrying a laser retro-reflector and, as an experiment, the Prare system (Precise Range and Range Rate Equipment). After the failure of the Prare system due to a radiation damage the satellite laser ranging (SLR) measurements are the basis for the precise orbit determination.

ERS-1 is flying in a sun-synchronous circular orbit (quasi-polar) at a mean altitude of 785 km and an inclination of 98.5 degrees with different ground repeat cycles (see table 1). The Kepler period is about 100.5 min.

To keep the satellite ground tracks within  $\pm 1$  km deadband (first 6 months  $\pm 2$  km) so called maintenance manoeuvres have to be executed, which take place usually every two to four weeks depending mainly on the solar activity.

Figure 1: ERS-1 Satellite

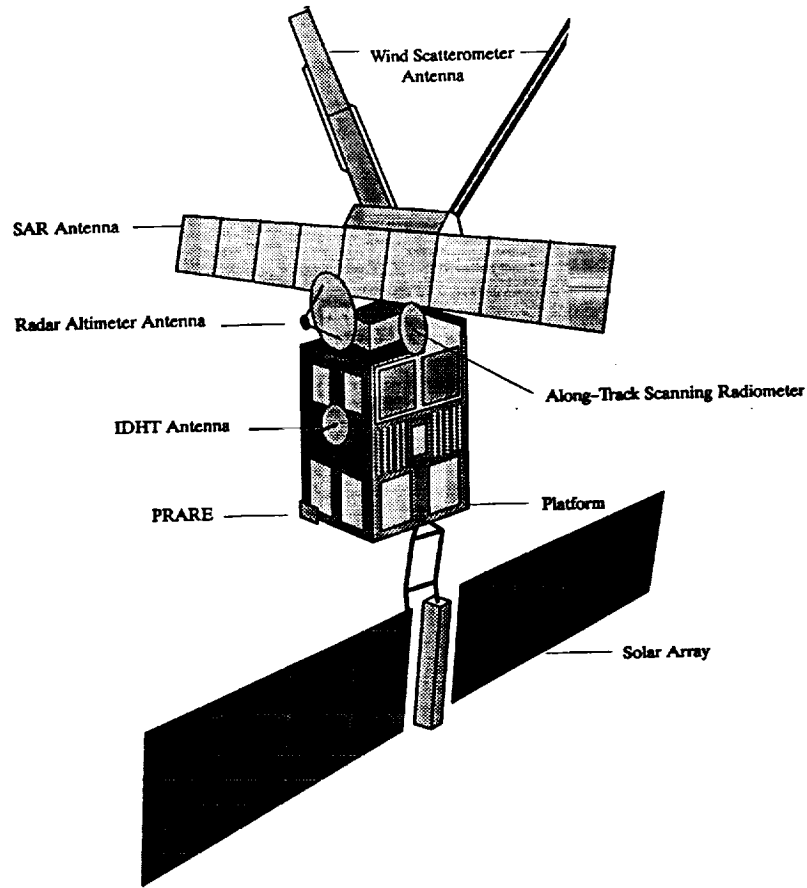


Table 1: ERS-1 Orbit Characteristics

	Repeat Cycle		
	3 days	35 days	176 days
Revolutions per cycle	43 revs	501 revs	2521 revs
Revs per day	14 + 1/3	14 + 11/35	14 + 57/176
Mean Semi-Major Axis [km]	7153.138	7159.4965	7156.30
Mean Inclination [Degrees]	98.516	98.5429	98.5114
Mean Eccentricity	1.165 x 10 <sup>-3</sup>	1.165 x 10 <sup>-3</sup>	1.165 x 10 <sup>-3</sup>
Mean Argument of Perigee	90.0 deg	90.0 deg	90.0 deg
Mean local solar time of descending node	10h 30min	10h 30min	10h 30min
Longitudinal phase (ascending node) [degrees]	24.36 East <sup>(1)</sup> 128.2 West <sup>(2)</sup>	20.9605 East	not decided
Duration	26/07/91-12/12/91 <sup>(1)</sup> 23/12/91-30/03/92 <sup>(2)</sup> 16/12/93-01/04/94 <sup>(2)</sup>	2/4/92-15/12/93	8/4/94-...

## 2. ERS-1 Laser Tracking Network

The ERS-1 satellite is tracked by a network of globally distributed stations which were funded by many different institutes. In table 2 the stations are listed along with their ERS-1 tracking periods.

In figures 2 to 4 the geographical distribution of the stations is plotted for the first three orbit phases (see table 1). As can be seen, most of the tracking stations are located in Europe and North America. The southern hemisphere is covered only by up to four SLR stations and none of them is located in the south African region. The plots show also the actual tracked ERS-1 orbital passes.

Figure 2: SLR Tracking Coverage within the Commissioning Phase (Venice Orbit)

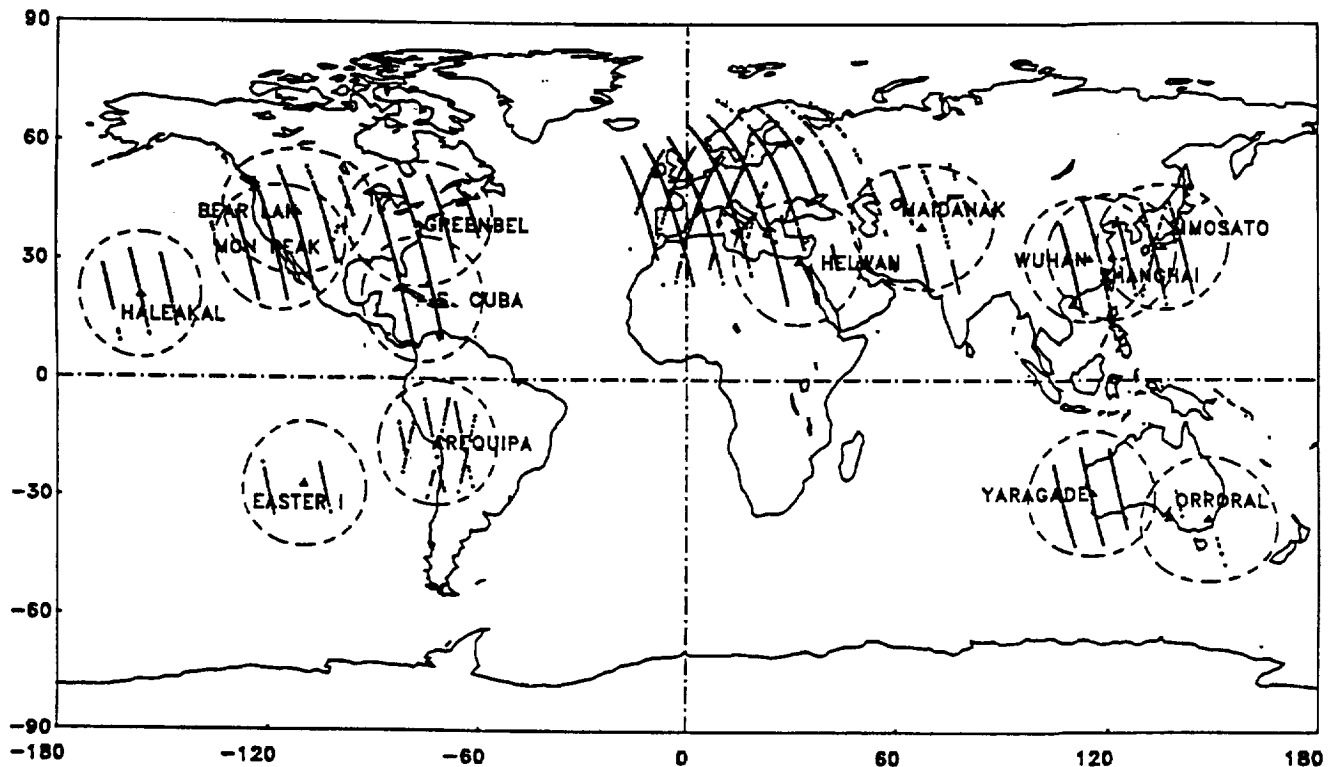


Table 2: ERS-1 Tracking Network Stations

ID	Name	Location	System	Tracking Periods
1181	Potsdam	Germany, Europe	fix	910720 ..
1863	Maidanak	Russia,	fix	910724 ..
1864	Maidanak	Russia,	fix	920421 ..
1873	Simeiz	Russia, Europe	fix	910723 .. 910829
				920501 ..
1884	Riga	Latvia, Europe	fix	910731 .. 911028
				920225 .. 920226
				920401 ..
1893	Katzively	Russia, Europe	fix	920422 .. 920515
1953	Santiago de Cuba	Cuba, Carribean	fix	910808 .. 910922
				911127 ..
7046	Bear Lake	USA, North America	TLRS-4	910906 .. 911015
7080	Fort Davis	USA, North America	fix	910822 .. 910822
				911121 .. 920124
				920318 ..
7090	Yarragadee	Australia	MOBLAS-5	910731 ..
7097	Easter Island	Chile, Pacific	TLRS-2	911018 .. 920311
7105	Greenbelt	USA, North America	MOBLAS-7	910802 ..
7109	Quincy	USA, North America	MOBLAS-8	911211 ..
7110	Monument Peak	USA, North America	MOBLAS-4	910725 .. 920306
				920504 ..
7210	Haleakala	Hawaii, USA	fix	910731 ..
7236	Wuhan	China, Asia	fix	910929 .. 920222
				920404 ..
7403	Arequipa	Chile, South America	TLRS-3	910731 .. 911010
7512	Kattavia	Greece, Europe	MTLRS-1	920328 .. 920426
7542	Monte Venda	Italy, Europe	MTLRS-2	910729 .. 910917
7810	Zimmerwald	Switzerland, Europe	fix	910719 ..
7811	Borowiec	Poland, Europe	fix	910807 .. 910818
				911002 .. 911006
				920107 .. 920121
7824	San Fernando	Spain, Europe	fix	911029 .. 920327
				920505 ..
7831	Helwan	Egypt, North Africa	fix	910803 .. 911131
				920226 ..
7835	Grasse	France, Europe	fix	910717 ..
7837	Shanghai	China, Asia	fix	910816 ..
7838	Simosato	Japan, Asia	fix	910720 ..
7839	Graz	Austria, Europe	fix	910722 ..
7840	Herstmonceux	Great Britain, Europe	fix	910719 ..
7843	Orroral	Australia	fix	910725 .. 910729
				911117 .. 911117
				920119 .. 920127
				920414 ..
7882	Cabo San Lucas	Mexico	TLRS-4	920319 ..
7883	Ensenada	Mexico	TLRS-4	911113 .. 911126
				920109 .. 920208
7907	Arequipa	Chile, South America	fix	911129 .. 911129
7918	Greenbelt	USA, North America	TLRS-3	920107 .. 920115
				920404 ..
7939	Matera	Italy, Europe	fix	910724 ..
8834	Wetzell	Germany, Europe	fix	910918 .. 910918
				920305 ..
MOBLAS	mobile laser system			
MTLRS	modular transportable laser system			
TLRS	transportable laser system			



Figure 3: SLR Tracking Coverage within the First Ice Phase (Ice Orbit)

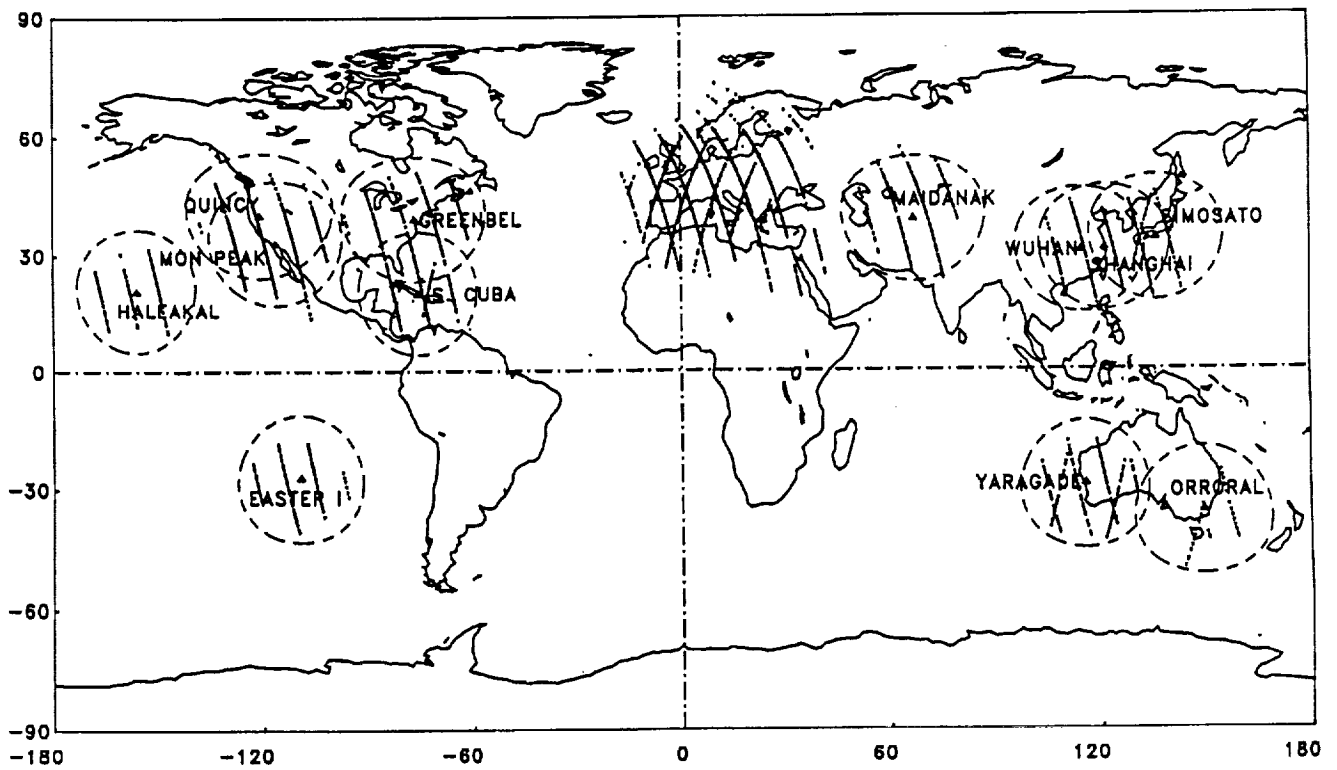
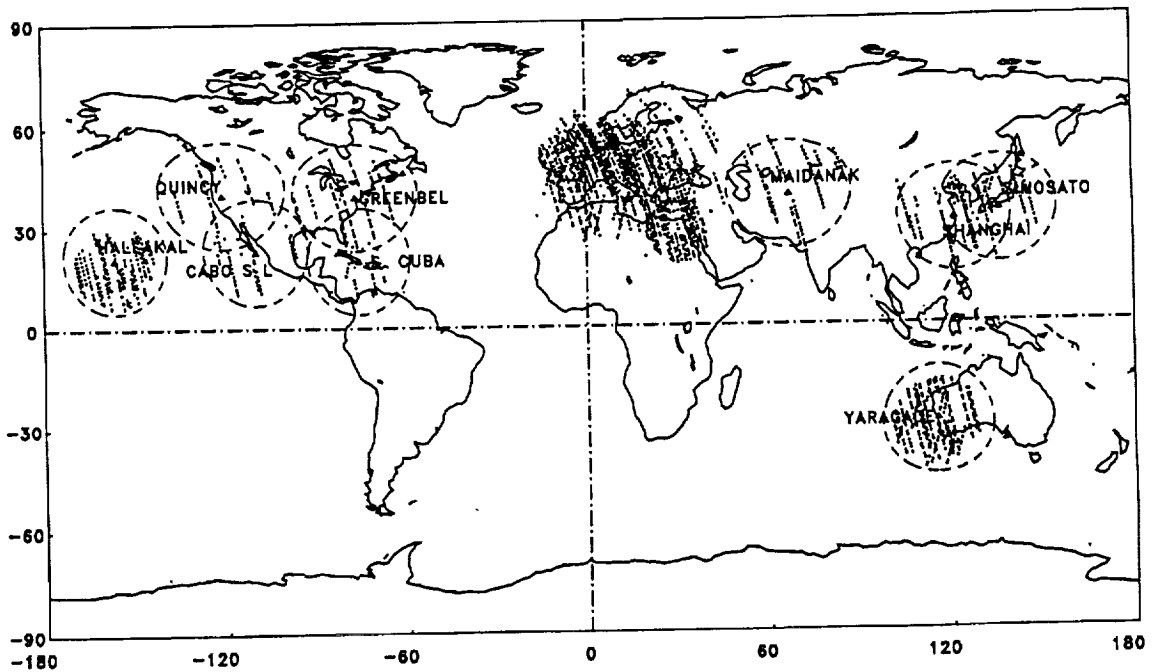


Figure 4: SLR Tracking Coverage within the first Month of the Multidisciplinary Phase



### 3. Data Flow to D-PAF Systems

Soon after the tracking of a satellite pass the SLR data is preprocessed at the station:

- a first data screening is performed by most of the stations;
- then from each pass about 50 data points were selected (quick-look (Q/L) data) or
- the measurements were compressed into onsite normal points (ONP).

This Q/L or ONP data is then transmitted to the Data Analysis Center at D-PAF. There are two centers collecting and forwarding the data: the data from the CDSLRL stations is transmitted via existing internal links to the CDSLRL headquarters and then forwarded to CDDIS; the second center is at the European Data Center (EDC) at DGFI. EDC is collecting all data from the European systems (EUROLAS) and also from stations in Russia, Cuba and China. From these two data centers D-PAF is retrieving the collected data files on a daily basis and merges them with data from those stations which have sent their data directly to D-PAF.

The data transmission is performed by using all currently available communication links: telex, Span, Bitnet, Internet, GE/MARK III and ftp.

After having applied all necessary corrections the full tracking data set (full-rate (FR)) is transmitted to the two centers, usually by CCT or Span. Again D-PAF retrieves the FR data sets from CDDIS and EDC and merges them with the directly received files.

It has to be noted, that all three parties exchange their data to have the full information available for all partners. In the beginning of the mission when EDC was not established D-PAF performed the EDC activities too.

According to the work distribution between the four European processing and archiving facilities (PAF) D-PAF is responsible for the generation of operational precision orbital products and for a processing of SAR data. In order to fulfill these tasks D-PAF has set up a number of processing systems. Used for the orbit generation are:

- the telecommunication system (TCS)
- the data management system (DMS)
- the **tracking and orbit determination system (TOS)**, which consists of the following subsystems:

**preprocessing** subsystem: preprocessing of incoming data, generation of normal points from laser and altimeter data

**orbit determination** subsystem: differential orbit correction by numerical integration methods, quality control, generation of numerical and graphical products

**orbit prediction** subsystem: orbit extrapolation, generation of orbit prediction sets in different formats, generation of time bias functions, quality control

**earth gravity modelling** subsystem: processing of surface gravity data, reduction and solution of normal equation systems, quality control

#### 4. Station Performance

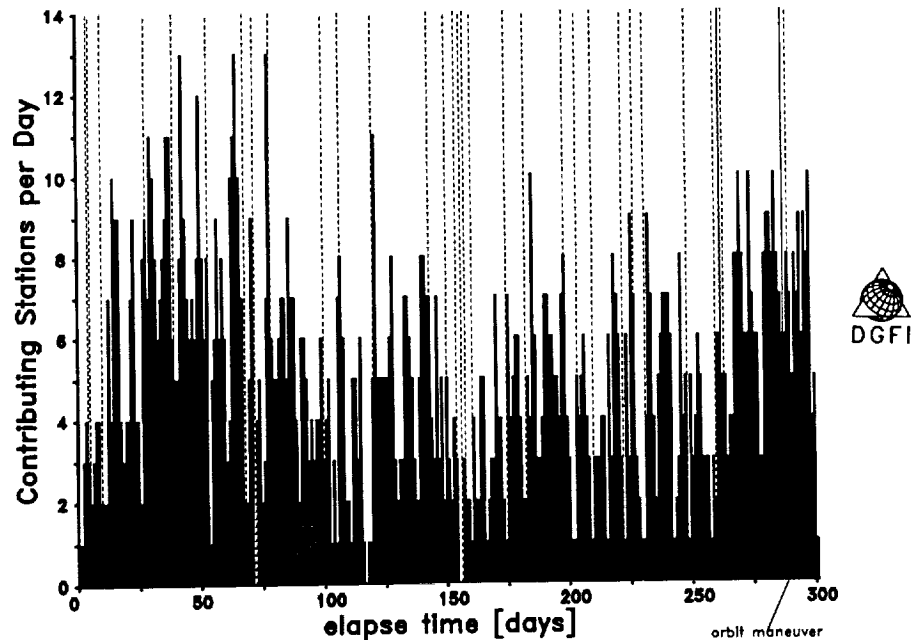
At D-PAF all incoming data is checked for quality and statistics are generated. On a weekly basis Q/L reports are generated presenting incoming data statistics and data quality check information. This paragraphs will present some of the statistical information.

As already seen in figures 2 to 4 only a small part of the ERS-1 orbital path is observed by the ground stations and this is mainly located north of the equator. Especially over South America the situation became worse from the first to the second phase and in the first month of the multidisciplinary phase there is no tracking in that part of the world.

From the figures it is also visible that mainly the ascending arcs were observed by the stations, while only a few descending arcs were tracked. The reason probably is that the descending passes can be tracked only during daylight.

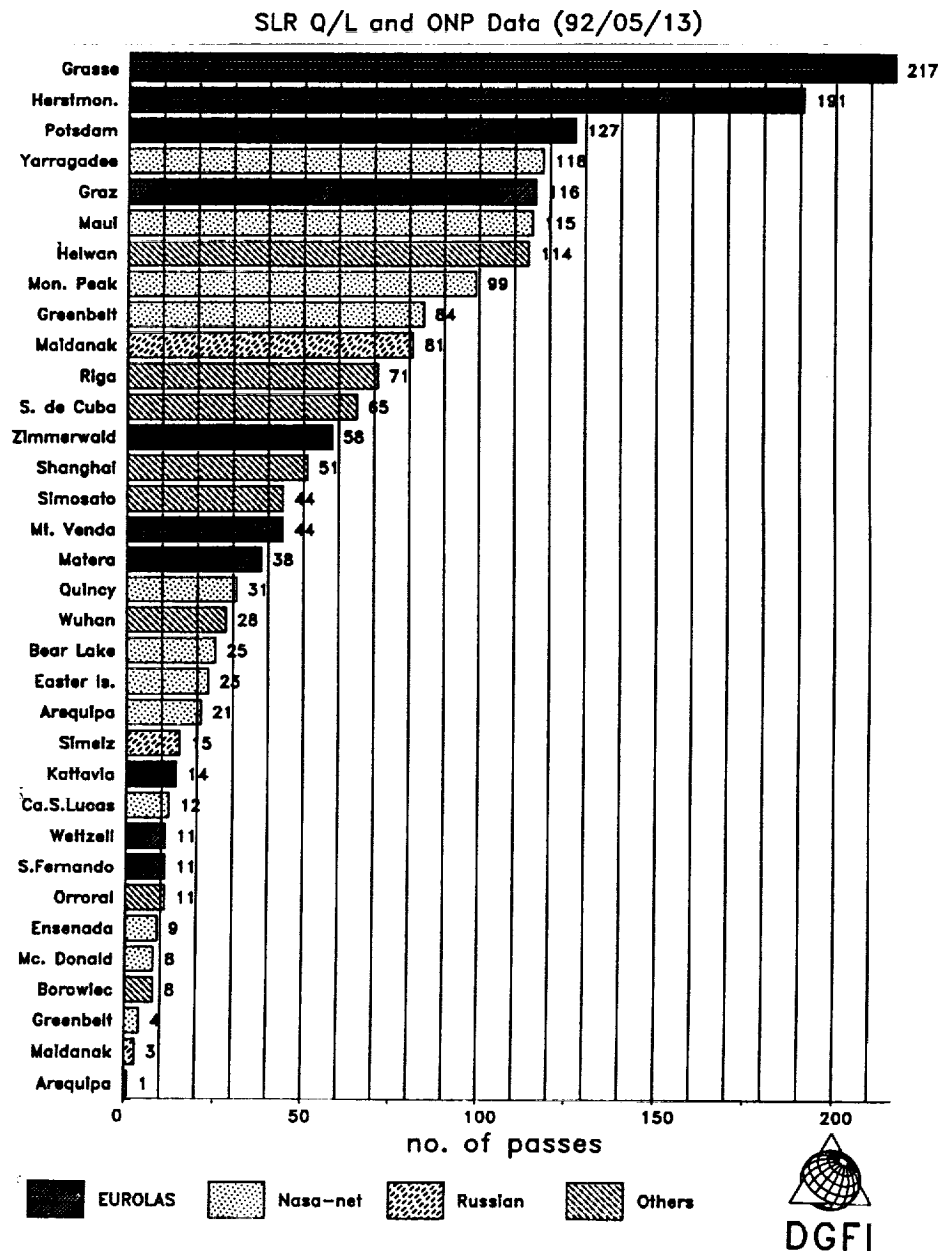
Figure 7 presents the variation in the number of stations observing ERS-1 per day. It ranges from 0 to 13 and shows clearly a decrease for the months October 91 to March 92, when ERS-1 was not in sunlight for many of the stations. A corresponding trend is visible in figure 9 which depicts the number of passes per week. For an arc of 7 days about 30 to 60 passes are available.

Figure 7: ERS-1 SLR Stations per Day



There is also a wide range in the number of passes being tracked by different stations. As can be seen from figure 8 this varies from 1 to 217. But one has to keep in mind that not all stations were continuously tracking, some were occupied only for a short while (e.g. Monte Venda, see table 2). The tracking contribution of some stations to the total ERS-1 tracking ranges from a few percent to almost 15 percent (Grasse).

Figure 8: Acquired ERS-1 SLR Passes per Station



Not only the data quantity is varying from station to station, but also the data quality is different. There are some stations with single shot precision of about 20 cm and others with 1 cm and less. Figure 10 depicts the station performance in terms of single shot and 15 sec. normal point accuracy for some stations.

Figure 9: Acquired ERS-1 SLR Passes per Week

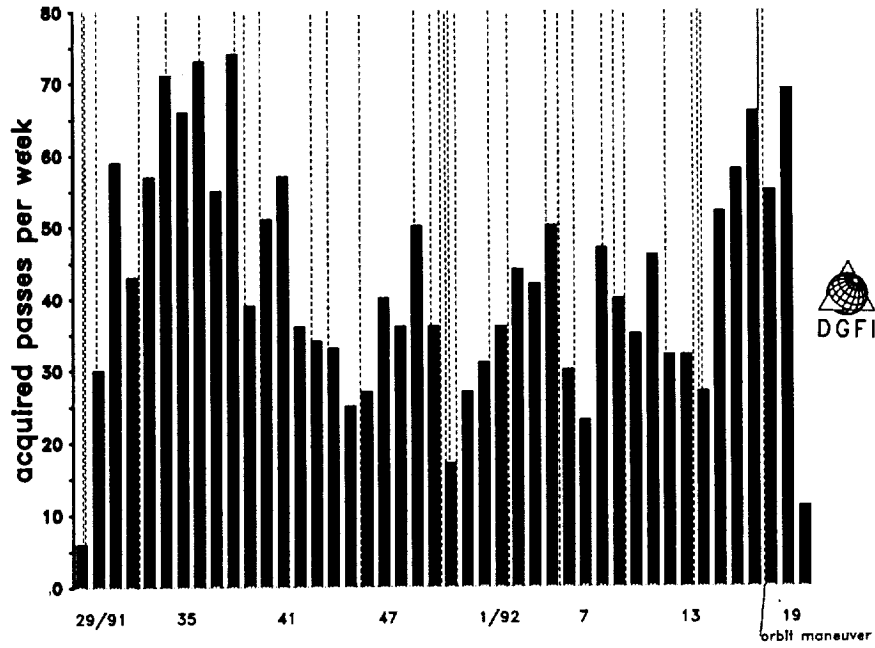
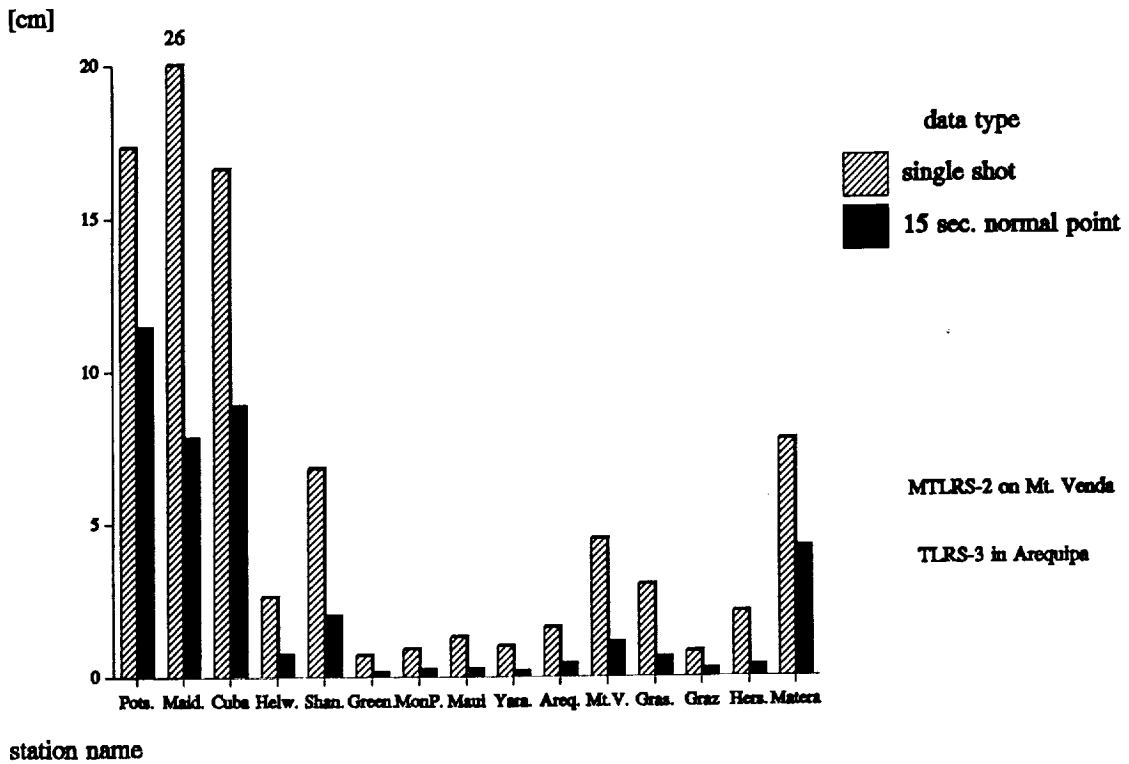


Figure 10: ERS-1 Tracking Precision per Station (cm)



## 5. Orbit Determination at D-PAF

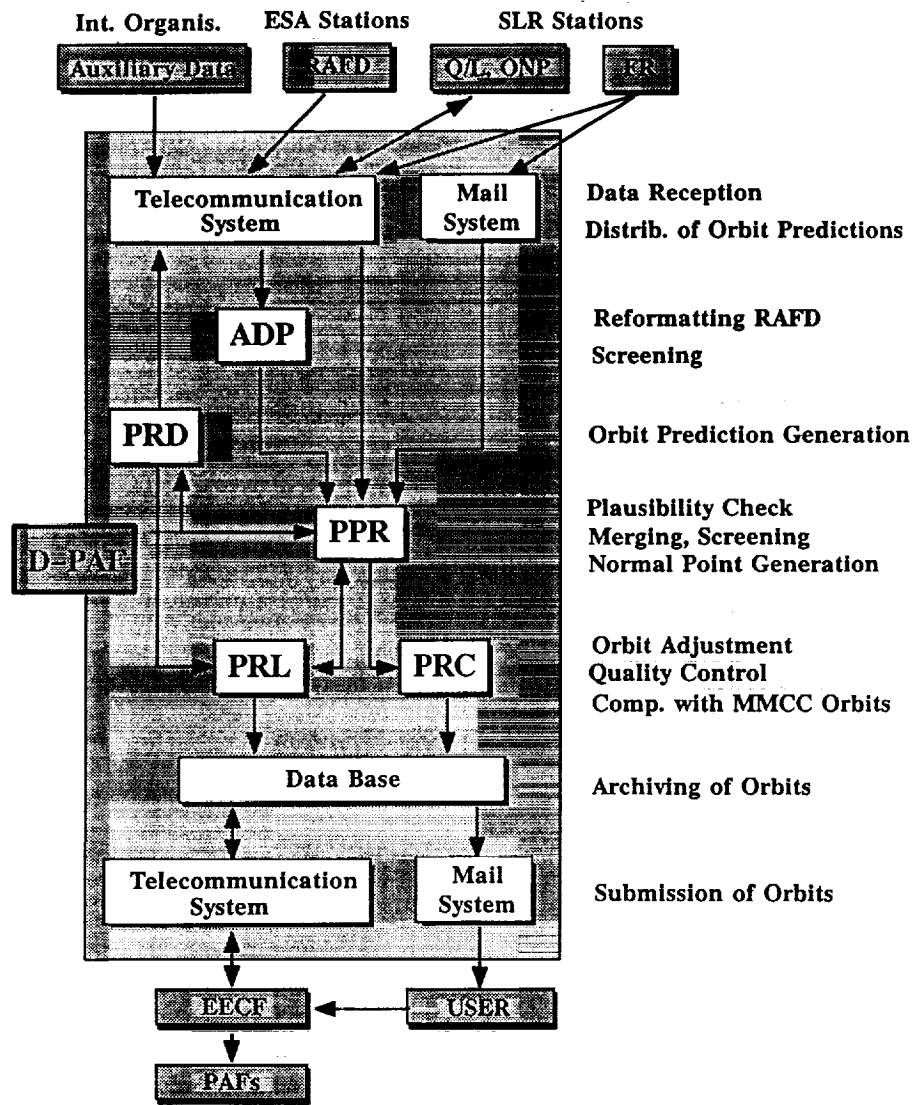
In order to provide ERS-1 precision orbits the following ERS-1 orbital products are routinely generated and distributed:

- orbit predictions and time bias functions
- preliminary orbits
- precise orbits

The latter two products are official ESA products, while the first one is an internal one. More details about the ERS-1 orbit predictions can be found in König et.al. (1992). A detailed description of all radar altimeter and tracking data products is presented in Bosch et.al. (1990).

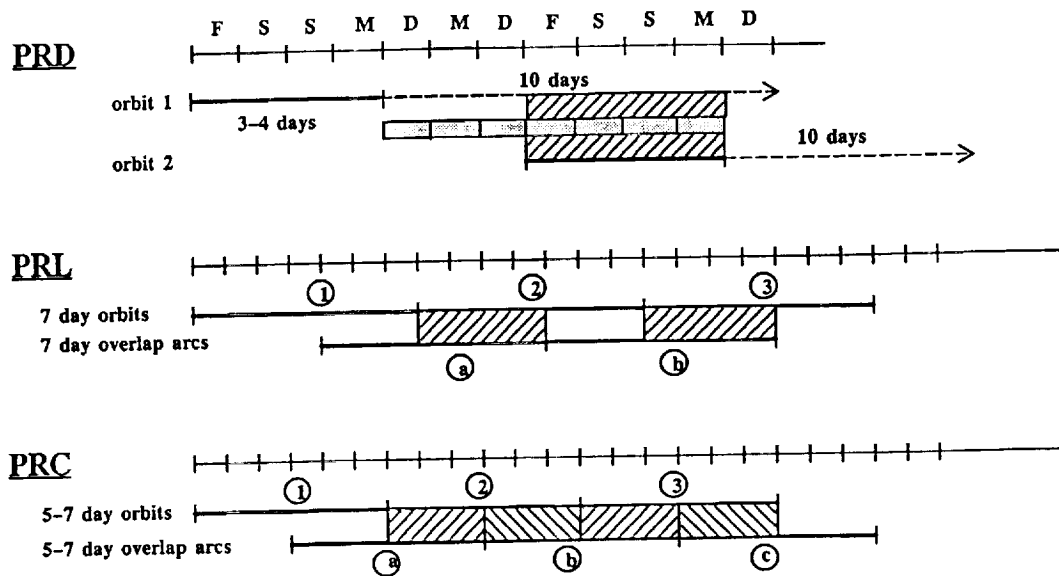
The overall data flow for the orbit determination processes is explained in figure 11.

Figure 11: Orbit Determination Data Flow



The processing schemes are outlined in figure 12 for manoeuvre free periods.

Figure 12: Processing Scheme  
(for manoeuvre free periods)



### 5.1 Preliminary Orbit Determination

Preliminary orbits are computed on a weekly basis by using Q/L laser and radar altimeter fast delivery (RA-FD) data and are usually available within two weeks. Both data sets are compressed into normal points (15 sec. bins for SLR, 10 sec. bins for RA-FD) after first quality checks. As can be seen from figure 14, the use of RA-FD data improves the global coverage especially for arc with only a few SLR passes.

In manoeuvre free periods weekly arcs are computed plus another 7-day arc which is overlapping by 3-4 days and is used for quality assessment (see figure 12). The models for the orbit determination are described in Zhu and Reigber (1991) and Massmann et.al. (1992). Solve-for parameters are the six orbital elements at epoch, one solar radiation coefficient, daily/half-daily drag coefficients, altimeter range bias (if RA-FD data is used) and station coordinates (for new stations only).

The resulting orbital fits are usually around 50-80 cm, in case of bad data coverage up to 130 cm. Figure 13 presents the quality control results from overlapping arcs for 1991 and 1992. The large values in November 91 are resulting from a period with no useful RA-FD data and only a very few laser passes. The same hold for the end of December 91.

Figure 13: PRL Precision Assessment by Overlapping Arc Comparison

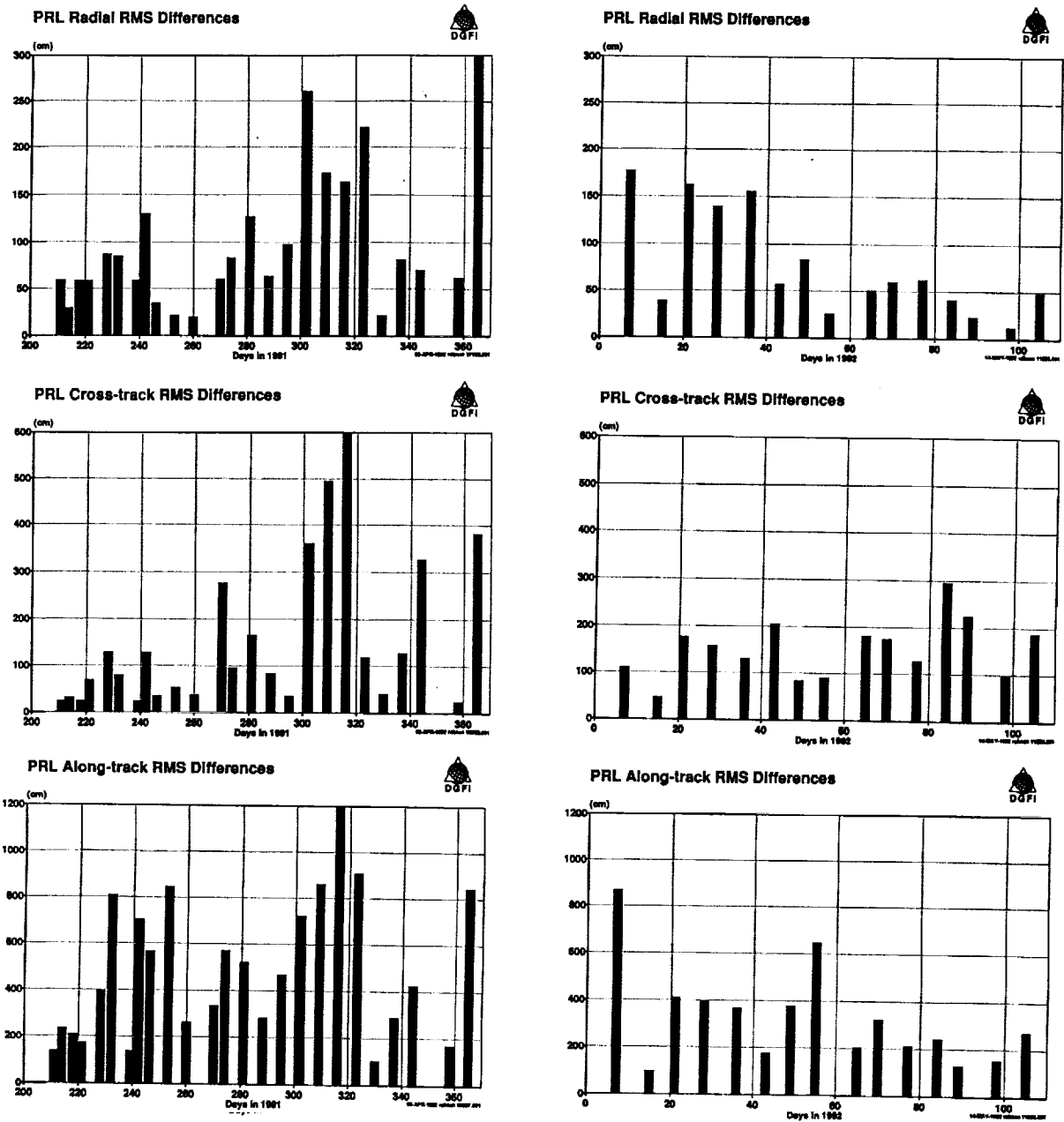
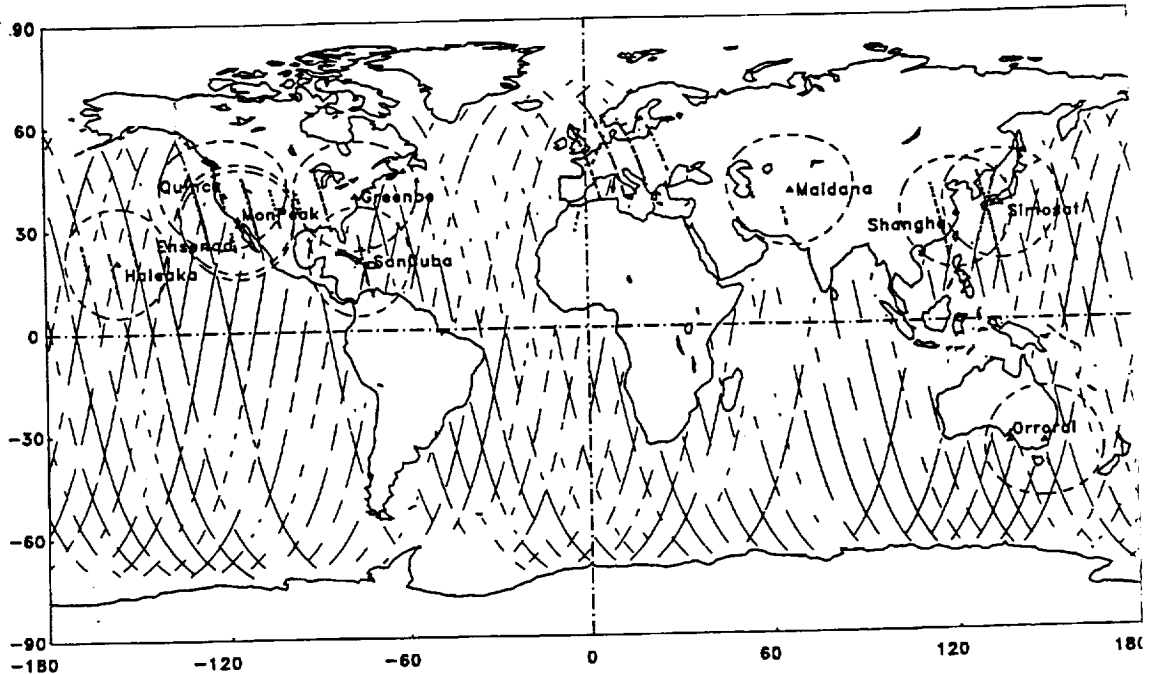




Figure 14: Input Example for the Preliminary Orbit Determination  
(January 20-27, 1992)



## 5.2 Precise Orbit Determination

The precise orbits are based up to now only on laser data which have been compressed into 15 sec. normal points. The orbits are computed with a delay of 3-6 months depending on the availability of all FR laser data at D-PAF. The arc length is chosen to fit as good as possible in between two manoeuvres and is usually in the range of 5-7 days. The quality control is also performed by overlapping arc comparison. Models and solve-for parameters are the same as for the preliminary orbits, except the earth rotation parameters, the geomagnetic indices and the solar flux data, which are now the official final values instead of predicted or preliminary ones.

Figure 15 presents the resulting rms orbital fit values for the precise orbit arcs generated up to now while figure 16 shows the quality estimates from the overlapping arc comparison. When comparing figure 13 and 16 one has to be careful, because the arcs are not the same. But generally one can say that the PRC results are more homogeneous and do not show large spikes due to better input data and a more intensive data handling. The most interesting radial component of the orbit seems to be accurate to 50 to 60 cm.

Figure 15: PRC Orbital Fits

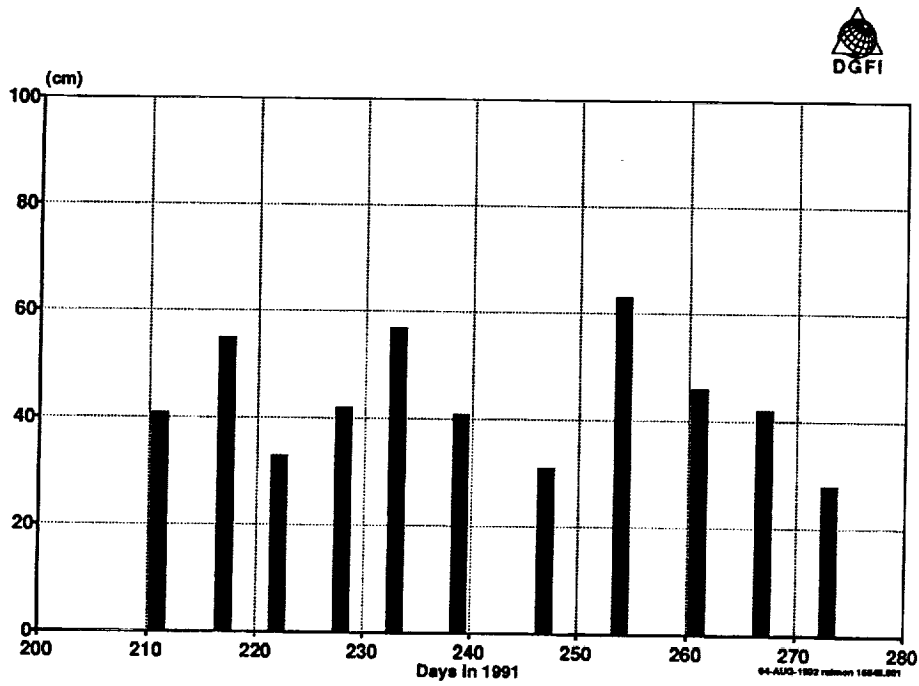
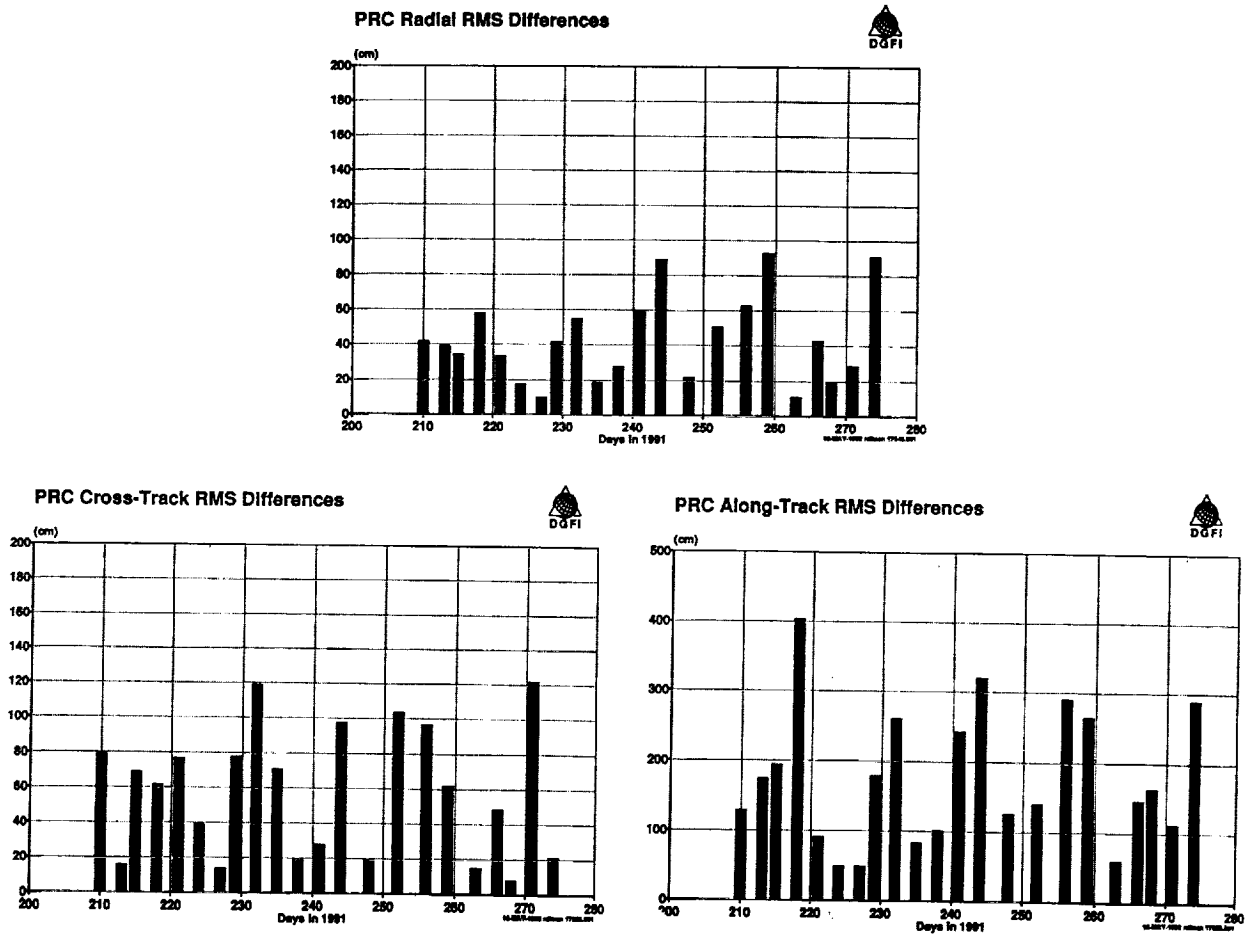


Figure 16: PRC Precision Assessment by Overlapping Arc Comparison



## 6. Conclusion

Soon after the ERS-1 launch DGFI/D-PAF has started the orbit computations and demonstrated its capability to generate good quality orbits on an operational basis. On the other hand the SLR stations have demonstrated their capability to track ERS-1 and provide high quality tracking data.

Nevertheless there are a few things that could be improved: The accuracy of the generated preliminary and precise orbits is very much limited by the spatial and temporal coverage of the SLR data.

Up to now there are only a few stations in the southern hemisphere of which only one has a good tracking record. On the African continent only one tracking station can be found and that is located in North Africa (Helwan). On the northern hemisphere some gaps can be identified over Russia.

The temporal coverage suffers from the fact that mostly the ascending ERS-1 arcs (night passes) were tracked by the stations. A reason for that is partly the missing daylight tracking capability of the station, partly tracking restrictions and partly man power problems.

Due to the data coverage it is difficult to model large ERS-1 drag perturbation, especially during periods with high solar activity. Tests are initiated to improve this by using either drag information derived from Spot2 Doris data or by using crossover altimeter data.

## References

- Bosch, W., Flechtner, F., König, R., Massmann, F.-H., Reigber, Ch., Schwintzer, P. and Wilmes, H., 1990. **The German PAF for ERS-1: RAT Product Specification Document.** D-PAF/DGFI, Document ERS-D-PSD-30000, Issue 1.1, München.
- König, R., Li, H., Massmann, F.-H., Raimondo, J.C. and Reigber, Ch., 1992. **On the Accuracy of ERS-1 Orbit Predictions**, this proceedings
- Massmann, F.-H., Reigber, Ch., Raimondo, J.C. and Rajasenan, C., 1992. **Operational ERS-1 Orbit Determination at D-PAF**, Proceedings of the Sixth International Geodetic Symposium on Satellite Positioning, Columbus, Ohio
- Zhu, S.Y. and Reigber, Ch., 1991. **The German PAF for ERS-1: ERS-1 Standards used at D-PAF.** D-PAF/DGFI, Document ERS-D-STD-31101, München.

## Laser ranging application to time transfer using geodetic satellite and to other Japanese space programs

Hiroo KUNIMORI\*, Fujinobu TAKAHASHI\*, Toshikazu ITABE\*  
and Atsushi YAMAMOTO\*\*

\* Communications Research Laboratory, 4-2-1 Nukui-kita, Koganei-shi,  
Tokyo 184 Japan

\*\* Maritime Safety Academy, Wakaba-Cho 5-1 Kure-shi, Hiroshima 737 Japan

### ABSTRACT

Communications Research Laboratory (CRL) has been developing a laser time transfer system using a satellite laser ranging (SLR) system. We propose Japanese geodetic satellite 'AJISAI', launched in 1986 as a target satellite. The surface is covered not only with corner cube reflectors but also with mirrors. The mirrors are originally designed for observation of flushing solar light reflected by the separate mirrors while the satellite is spinning. In the experiment, synchronized laser pulses are transferred via specified mirror from one station to another during the satellite is up on the horizon to both stations. The system is based on the epoch timing ranging system with 40 ps ranging precision, connected together with UTC(CRL). Simulation study indicates that two stations at thousands of km distance from each other can be linked with signal strength of more than 10 photons and the distributed images of laser beam from AJISAI mirrors give many chances to two stations to link each other during a single AJISAI pass.

In other topics on the application to Japanese space programs, Retro-reflector In Space for Advanced Earth Observation Satellite (ADEOS) and RendDezVous docking mission of Experimental Technology Satellite-VII (ETS-VII) are briefly presented.

### 1. Laser Time Transfer via Geodetic Satellite AJISAI

#### 1.1 Introduction

Users of time and frequency standards have been able to take a variety of time comparison techniques even if they pursue the highest accuracy. The precision of GPS common view observation, for example, have got to several few nano seconds and 1 ns or higher precision have been attained by radio techniques such as two way time transfer via satellite (Ref.1). The requirement of such an extremely high precision may exist in deep space navigation, space geodesy, relativity physics and astronomy which always demand extreme precision and accuracy in their measurements. In addition to the radio techniques, time transfer using optical pulses has recently been suggested as one of potential for giving precision of sub-nano or picosecond time transfer to overcome the maximum bandwidth of radio waves (Ref.2).

Satellite laser ranging (SLR) have progressed as one of space geodetic techniques in the field of global geodesy and geophysics. Some SLR stations measure the range to as precise as 30 ps or higher (Refs. 3,4). Since the SLR system is essentially a highly precise epoch recorder transmitting and receiving of optical pulses, a combination of two or more SLR systems has potential as a highly precise time comparison and transfer system.

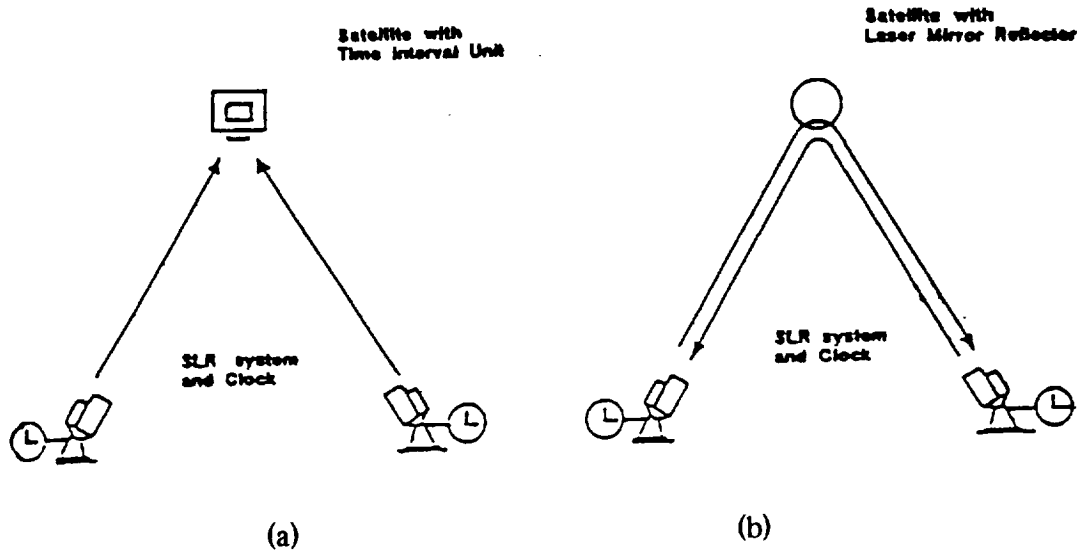


Fig.1 Configuration of Laser time transfer  
 (a) One way uplink (LASSO) (b) Two way

There are two configurations considered for ground-based-laser time transfer system using a satellite (See Fig.1). The first is called the one-way up-link configuration. Both SLR stations transmit a laser pulse to the time interval unit (TIU) on the satellite and the TIU measures the interval between their arrival times. Such an optical time comparison has been performed in Europe in the LASSO experiment (Refs. 5,6). In the LASSO experiment of European phase, laser echoes were successfully received at Grasse, France and at other European laser ranging sites. The second is the two-way configuration. Each station transmits a laser pulse to the other station via a satellite with mirror reflectors. The satellite also has corner cube reflectors for conventional SLR, and they are used to determine the distance from each station to the satellite to give support to the time transfer solution. In this paper, we examine the two-way configuration using the Japanese SLR satellite AJISAI, including time transfer concept, calibration methods, signal strength and spatial distribution of the reflected beam. The system performance is based on the CRL SLR system (Refs. 7,8), including additions to be made for two-way time transfer.

### 1.2 Target satellite AJISAI

Table 1 : Major specifications of AJISAI

Launch Date: August, 1986	
Configuration: Polyhedron inscribed in sphere of diameter 2.15 m	
Weight: 685kg	
Corner cubes: 1436 pieces,	Effective area :91.2 cm <sup>2</sup>
Number of mirrors :318 pieces,	Curvature of mirrors :8.4-9 m
Reflective efficiency: 0.85,	Brightness : 1.5-3.5 star mag.
Duration of a flash : . 5 msec,	Rate of flashing : 2 Hz
Spin rate: 40 rpm	
Launch orbit: Altitude 1500 km,	
Inclination 50 deg,	Eccentricity 0.001

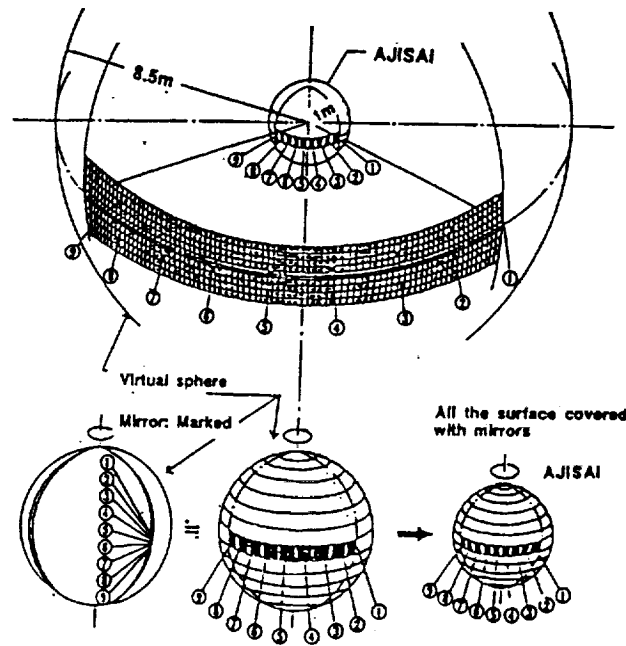


Fig.2 Arrangement of mirrors on AJISAI  
Parts of an 8.5m radius virtual sphere (mirror) is placed on the surface of the 1-m radius AJISAI maintaining their latitude angles.

AJISAI is the Japanese geodetic satellite launched in 1986 by the National Space Development Agency (NASDA). The major specifications of AJISAI are listed in Table 1. The satellite is a hollow sphere 2.15 m in diameter and weighs 685 kg. The surface is covered with mirrors as well as corner cube reflectors. The orbit is a circular with an inclination of 50 degrees and an altitude of 1500 km (Ref.9). The mirrors were originally designed for observing flashing solar light reflected by separate mirrors while the satellite is spinning at about 40 rpm. Each mirror is a piece of a surface with a radius of curvature of 8.5 m. Three elements from the same latitude of the 8.5-m sphere at longitudes of 0, 120 and 240 degrees are put on the surface of a 1-m radius satellite retaining the phase angle of the original sphere (See Fig.2). The latitudes from which every set of three is taken are uniformly selected from the original surface so that a distant observer can observe the light reflected from the front surface flashing three times per rotation.

### 1.3 Two way time transfer

The equation for two-way time transfer via laser pulse is in principle the same as those being developed in radio frequency band (Ref. 1). The time difference  $d_{12}$  (: positive when clock 1 is ahead of clock 2) between the clocks of stations 1 and 2 is given by:

$$d_{12} = (t_{21} - t_{12} + t_1 - t_2) / 2 + (R_{12} - R_{21}) / 2c \quad (1),$$

where :  $(i, j = 1, 2)$ ,

$t_i$  : Epoch of pulse departure at station  $i$  measured by station clock  $i$ ,

$t_{ij}$  :  $(i, NE, j)$  Epoch of station  $i$ 's pulse reflected by a satellite mirror arriving at station  $j$  measured by station clock  $j$ ,

- $R_{ij}$ : ( $i, NE, j$ ) One-way distance of a laser pulse to travel from station  $i$  to station  $j$  via the satellite, and  
 $c$ : speed of light.

The last term  $(R_{12}-R_{21})/2c$  is expected to be nearly zero because of the good symmetry of travelling paths, but not negligible due to the effect on motions of both satellite and stations. It is related to the difference between the satellite position at the times the two laser pulses arrive. It approaches zero if the two pulses arrive at nearly the same time on the satellite. This is done by controlling the firing timing at both stations. Timing control within the precision of 1-ns is necessary to obtain a station to station link by a mirror of AJISAI with 20cm x 20cm size spinning at 40 rpm. If the laser fire timing is controllable to 1 $\mu$ s,  $(R_{12}-R_{21})/2c$  is down to a few ps on the assumption that both the predicted position of the satellite and the clock synchronization are known with the accuracy of less than 1  $\mu$ s (300 m in distance) before the experiment. The  $\mu$ s firing control can be performed by a fully active mode-locked laser operation. In this observation mode, we can apply the geometric method rather than dynamical one to the orbit solution using SLR range data (Ref.10).

#### 1.4 Laser ranging system

We use an active-passive mode-locked Nd:YAG laser to generate 532 nm wavelength optical pulses 100 ps wide. The passive mode-locking is performed by saturable dye. The energy is 100 mJ per pulse and the nominal repetition rate is 10 pulses per second. The repetition rate can be controlled from 7 to 14 pps by real-time software. If the passive mode-locking by a saturable dye is replaced with an active component, the synchronization of firing timing can be controlled on nanosecond level (Ref.11).

The receiving telescope aperture has diameter of 1.5 m. A micro-channel plate photo multiplier (MCP-PMT) is used for detector. It has a 300-ps rise time, 8% quantum efficiency and the transit time jitter of less than 30 ps with a constant fraction discriminator. The MCP detector can be also gated temporarily by the prediction of photons arrival in 20-ns time steps.

The timing system consists of a high performance disciplined quartz oscillator, a GPS receiver, and a time interval unit (TIU). Either a GPS timing receiver or cesium clock of UTC (CRL) can keep the reference to UTC. Timing epoch is measured for up to 4 stop events with a resolution of 40-ps.

#### 1.5. Calibration system

In the actual experiment, we must consider that the reference signal of the atomic clock is transmitted to the SLR system via cables and electronics. Furthermore, the laser transmitting and receiving point is not at the telescope reference point.

The cables and electronics delay between the atomic clock and the TIU is monitored by an independent measurement system. Figure 3 is a block diagram of the monitoring system used in the experiment. The combined 5-MHz+1-pps signal from the cesium clock room is transmitted via a 500-m optical fiber. Output signal (50 MHz) of the quartz oscillator is phase-locked by the 5-MHz and used as the reference frequency in TIU. The 1 pps signal is used for the epoch reference of UTC. The 5-MHz and 1-pps signals are combined again at SLR site and are sent back to the clock room. Then delay and phase difference with respect to the original signals are continuously monitored at the clock room. It has been installed to get the characteristics of the long-term stability of the system.

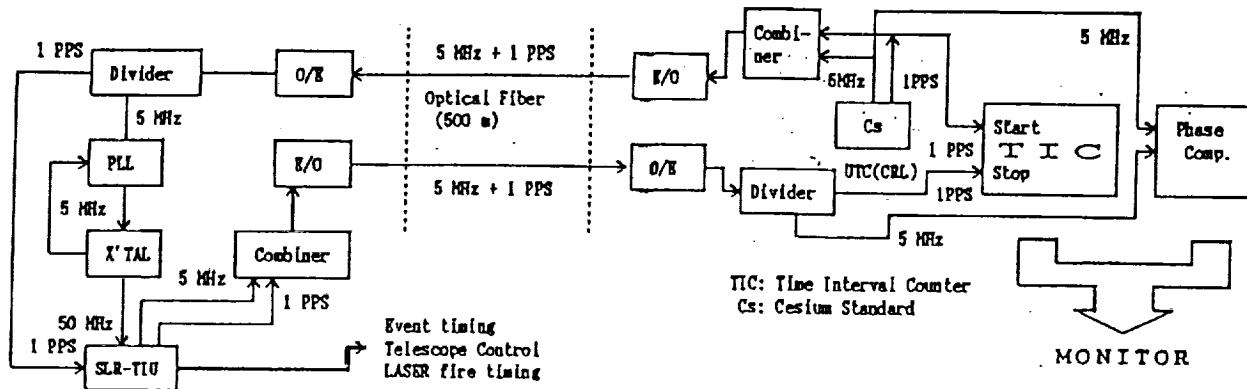


Fig.3 Reference signal monitoring system

The epoch latch point at each laser pulse start and stop must be treated as if these events occurred at the telescope reference point ( intersection of two rotation axes). The calibration target is put on the telescope moving axis, as it takes partial reflection of transmitting beam and its physical distance from reference point must be measured precisely.

The time difference between clocks including calibration term ( $d'_{12}$ ) is given by:

$$d'_{12} = (t_{21} - t_{12} + t_1 - t_2) / 2 + (R_{12} - R_{21}) / 2c + \{ (t_{1a} - t_{1b}) - (t_{2a} - t_{2b}) + (t_{2x} + t_{2y}) - (t_{1x} + t_{1y}) \} / 2 \quad (2),$$

where : ( $i=1,2$ ), in addition to the parameter defined in Eq.1,

$t_{i,a}$  : Optical path delay from firing (laser input) point to telescope reference point at station  $i$ ,

$t_{i,b}$  : Optical path delay from telescope reference point to receiver point at station  $i$ ,

$t_{i,x}$  : Electronic delay from firing point to start-epoch latch gate at station  $i$ , and

$t_{i,y}$  : Electronic delay from receiver point to stop-epoch latch gate at station  $i$ .

In order to calibrate the time difference between clock 1 and 2, each value of parameter in { } in the Eq.2 must be evaluated. The optical delay can be measured by a distance meter or by scales, and it will be stable in time unless optical design is changed. To cancel out the electronic delay, the common portable receiver can be collocated at two stations. This measurement would still have errors coming from the dependence on signal strength and temperature.

### 1.6 Link budget

In the laser time transfer experiment, the number of photons ( $N_p$ ) detected at the remote ground station are calculated according to the following equation:

$$N_p = (E\lambda/hc) \cdot (r_1 r_2 f_s^2) \cdot (16A_s A_r \pi^2 R_1^2 R_2^2 q_i^2 q_s^2) \quad (3)$$

where  $E$  : Energy in a pulse,

$\lambda$  : Laser wavelength,

$h$  : Planck's constant,

$c$  : Velocity of light,

$r_1$  : Transmission beam efficiency,  $r_2$  : Receiving beam efficiency,



- $r_3$  : Target reflector reflectivity,
- $r_4$  : Atmospheric transmission efficiency (one-way),
- $A_s$  : Total reflector surface area,     $A_r$  : Received aperture surface area,
- $R_1$  : Station 1 to satellite distance,     $R_2$  : Station 2 to satellite distance,
- $q_t$  : Transmission beam divergence, and
- $q_s$  : Reflectors beam divergence for incident light return

Figure 4 shows the expected number of photons for AJISAI mirror reflection and the satellite elevation from stations, assuming the parameters have the values listed in Table 2. We also assume the position of AJISAI is roughly in the middle of the two station's common sky. From stations 2500 km apart, AJISAI is observed at above 40 degrees and more than 10 photons are expected.

**Table 2 : Parameters for estimating the number of photons**

Satellite Altitude	: 1500km (AJISAI)	
Energy of pulse (E)	: 100 mJ	
Wavelength ( $\lambda$ )	: 532 nm	
Transmission efficiency ( $r_1$ )	: 0.6	Receiving efficiency ( $r_2$ ): 0.3
Target reflectivity ( $r_3$ )	: 0.9	
Atmospheric transmission efficiency ( $r_4$ )	: 0.6	
Reflector surface area ( $A_s$ )	: 0.04 m <sup>2</sup>	
Received surface area ( $A_r$ )	: 0.27 m <sup>2</sup> (60cm aperture)	
Transmission beam divergence ( $q_t$ )	: 5 arcsec	

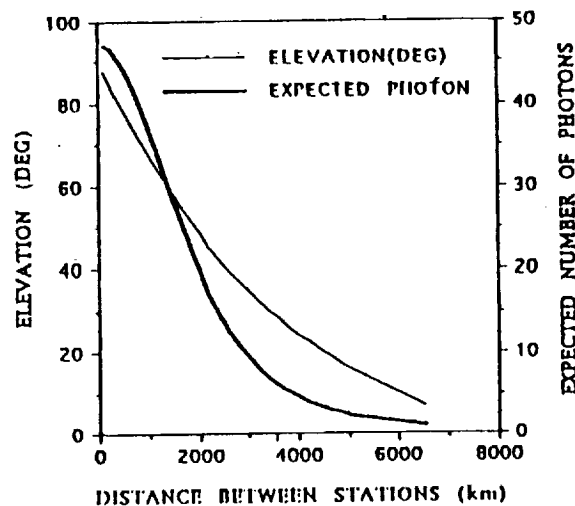


**Fig.4** Elevation and Expected number of photon v.s. distance between stations in laser time transfer via AJISAI

### 1.7 Spatial distribution of laser reflection

We simulate the spatial distribution of laser reflection from AJISAI to study the possibility of an optical link for time synchronization between stations. We calculate first the rotation phase and the incident angle of AJISAI for a given transmitting station and epoch, then project the image onto the ground from all mirrors visible to both stations. The calculation continues according to the given time step.

In Fig.5, each rectangle is the image of the laser reflection on the ground for an instantaneous laser shot and the number by the rectangle shows the reflector number on AJISAI. In Fig.6, three steps of 50 msec (one AJISAI spin) are illustrated successively.

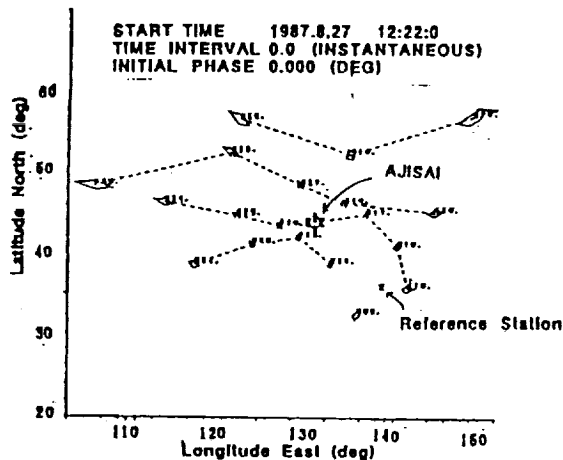


Fig.5 Instantaneous spatial distribution of reflected images on the ground via AJISAI mirror reflector. (The number next to each image indicates the mirror number on AJISAI)

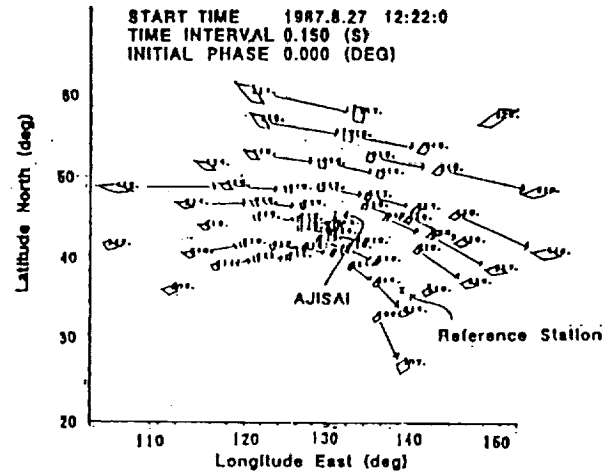


Fig.6 Spatial distribution of reflected images in three 50 msec steps. (The number next to each image indicates the mirror number on AJISAI)

A several percent of East Asia can locate an image, but there is a chance for many stations to get the link every AJISAI pass. If the timing of every shot is as accurate as the prediction, time comparison can be performed on average once every few seconds by simultaneously determining the rotation phase of AJISAI.

## 2. Application to Japanese Space Program

Table 3 lists the satellite name and its launching schedule in Japanese R&D space program. The schedule is released before the H-II rocket engine explosion which will cause at least one year delay shift from original schedule.

### 2.1 RIS

Retro-reflector In Space (RIS) is one of missions on ADEOS (Advanced Earth Observing Satellite) satellite which is scheduled for launch in 1996. The orbit is a sun synchronous sub-recurrent polar-orbit with an inclination of 98.6 deg. It has a period of 101 minutes and an altitude of approximately 800 km (Ref.12). RIS is a single element cube-corner

Table 3 R&D Satellite Launching Schedule (1992- 2001), released by NASDA in April 1992

Fiscal year/ Satellite name

1992	JERS-1, FMPT
1993	ETS-VI, SFU
1994	IML-2, SFU
1995	<u>ADEOS</u>
1996	COMETS
1997	TRMM, <u>ETS-VII</u>
1998	JEM-1,2, ADEOS-II
1999	JEM-n
2001	HOPE

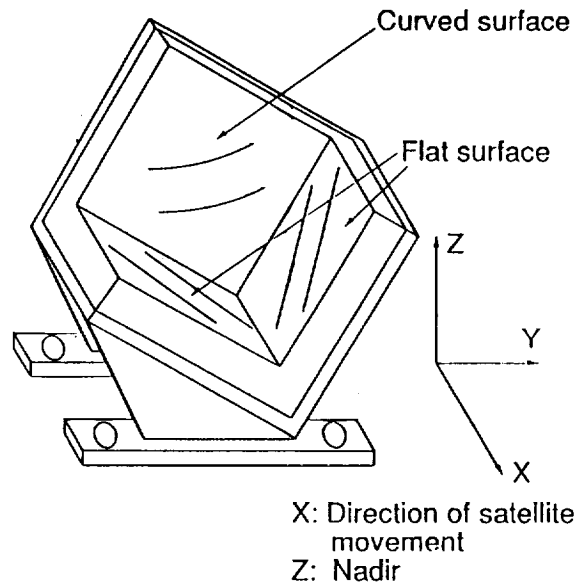


Fig.7 Structure of RIS  
( Effective diameter : 50cm )

retro-reflector with a diameter of 0.5 m designed for earth-satellite-earth laser long-path absorption experiments. RIS is proposed by the National Institute for Environmental Studies collaborated with CRL.

In the experiment, laser beam transmitted from a ground station is reflected by RIS and received at the ground station. The absorption of the intervening atmosphere is measured in the round-trip optical path. Figure 7 shows the structure of RIS. We use a slightly curved mirror surface for one of three mirrors forming the retro-reflector, which diverges the reflected beam to overcome the velocity aberration caused by the satellite movement.

We have proposed a simple spectroscopic method which utilizes the Doppler shift of the reflected beam resulting from the satellite movement for measuring the high resolution transmission spectrum of the atmosphere. The wider laser beam is used for illuminating satellite and for autonomous tracking the satellite by guiding camera.

## 2.2 ETS-VII

NASDA will schedule to launch the Experimental Technology Satellite (ETS-VII) in 1998 whose objectives are development of space robotics and rendezvous control. It consists of two satellites, the chaser and the target, each has GPS receiver for orbit control of chaser. Tentative altitude is 550km and communication to the ground will utilize the data relay satellite.

We have proposed that each satellite should be loaded with corner cube reflector set, one of which is two-color sensitive and be monitored the rendezvous process from the ground. We will track the satellites with switching or simultaneously mode depending on two satellites being within one beam or not.

## 3. CONCLUSION

We have studied the feasibility of the sub-nanosecond precision laser time synchronization system with a target satellite of AJISAI based on CRL laser ranging system, whose timing system is connected with UTC(CRL).

Simulation study indicates that two stations at thousands of km distance from each other can be linked by laser beam with signal strength of more than 10 photons. The images of laser beam from AJISAI mirrors is uniformly distributed on the ground and two stations have many chances to link each other during a single AJISAI pass. It requires the  $\mu$ sec control of laser fire timing, however, it bring on the precise information of the orbit as well by using the self-returned satellite range data.

The system has been operating in geodetic mode since CRL started the SLR observations to the major geodetic satellites from 1990. While global position of the SLR station has been determined with the precision of several centimeters, we are re-designing our system so that current system has also for time synchronization mode operation as well as adapting for Japanese space program in future.

### REFERENCES

1. Kirchner D.,1991, Two-way Time Transfer via communication satellites, Proc. IEEE, Vol.79, No.7, pp.983-990
2. Leschiutta S.,1991, Time synchronization using laser techniques, Proc. IEEE, Vol.79, No.7, pp.1001-1008.
3. Degnan J.J., 1985, Satellite Laser Ranging : Current Status and Future Prospects, IEEE Trans. Geosci. Remote Sensing, GE-23, 4, pp.398-413.
4. Pearlman M., & al. 1989 , Ground-based laser ranging measurement techniques and technology, Report of CDP-COOLFONT, section2.1, pp.1-26.
5. Serene B. and Albertinoli P. 1979, The LASSO Experiment, Proc.PTTI 11th conference, pp.145-167.
6. Veillet C. 1989, LASSO - the European Phase Aug.88-Sept.89, Proc.7th International Workshop on Laser Ranging Instrumentation, Matera 2-6 .
7. Kunimori H. & al. 1991, "Satellite Laser ranging system", Journal of CRL, Vol.38, No.2 ,pp.303-317 .
8. Greene B.A. 1984, Epoch timing for laser ranging, Proc. 5th International Workshop on Laser Ranging Instrumentation (Herstmoncex) , pp.247-250.
9. Sasaki M.and Hashimoto H. 1987, Launch and observation program of the experimental geodetic satellite of Japan, IEEE Trans.Geo.Rem., GE-25, 5, pp.526-533.
10. Yang F.M. 1986, The proposal of strictly simultaneous satellite laser ranging, The 6-th international workshop on laser ranging instrumentation, France, pp.549-557.
11. Electro Optic Systems 1991, EOS-V1 Active/Active Laser Characterization .
12. Sugimoto,A., Minato A. and Sasano Y.,1991, Retro-reflector in space for the ADEOS satellite, CREO'91 Baltimore.

## APPLICATIONS OF SLR

B.E. Schutz  
Center For Space Research  
The University of Texas at Austin  
Austin, TX 78712, USA

## INTRODUCTION

Satellite Laser Ranging (SLR) has a rich history of development which began in the 1960s with 10 meter-level first generation systems. These systems evolved with order of magnitude improvements to the systems that now produce several millimeter single shot range precisions. What began, in part, as an interesting application of the new laser technology has become an essential component of modern, precision space geodesy, which in turn enables contributions to a variety of science areas.

Modern space geodesy is the beneficiary of technological developments which have enabled precision geodetic measurements. Aside from SLR and its closely related technique, Lunar Laser Ranging (LLR), Very Long Baseline Interferometry (VLBI) has made prominent science contributions also. In recent years, the Global Positioning System (GPS) has demonstrated a rapidly growing popularity as the result of demonstrated low cost with high precision instrumentation. Other modern techniques such as DORIS have demonstrated the ability to make significant science contributions; furthermore, PRARE can be expected to contribute in its own right.

An appropriate question is "why should several techniques be financially supported"? While there are several answers, I offer the opinion that, in consideration of the broad science areas that are the benefactors of space geodesy, no single technique can meet all the requirements and/or expectations of the science areas in which space geodesy contributes or has the potential for contributing. The more well-known science areas include plate tectonics, earthquake processes, Earth rotation/orientation, gravity (static and temporal), ocean circulation, land and ice topography, to name a few applications.

It is unfortunate that the modern space geodesy techniques are often viewed as competitive, but this view is usually encouraged by funding competition, especially in an era of growing needs but diminishing budgets. The techniques are, for the most part, complementary and the ability to reduce the data to geodetic parameters from several techniques promotes confidence in the geophysical interpretations.

In the following sections, the current SLR applications are reviewed in the context of the other techniques. The strengths and limitations of SLR are reviewed and speculation about the future prospects are offered.

## SLR Summary

Satellite Laser Ranging measures the round-trip time-of-flight for a laser pulse to travel from a transmitter to a target and back. Current and near-term satellite targets include Starlette (1000 km

altitude), Ajisai (1500 km), ERS-1 (800 km), Lageos (59000 km) and Etalon-1 and -2 (25000 km). Future satellites include TOPEX/POSEIDON (August 1992 launch) and Lageos-2 (October 1992 launch). The geodetic satellites (Starlette, Ajisai, Lageos and Etalon) have a long orbital lifetime measured in thousands of years to millions of years for the high altitude satellites, thereby offering a distinct advantage that the satellite will be available at no cost for a very long period of time. Only the ground segment requires operation and maintenance support. By contrast, all other satellite techniques (GPS, DORIS, PRARE) rely on an active space segment with a lifetime determined by the on-board power system, usually several years. VLBI, on the other hand, uses extragalactic radio sources which will, presumably, be available for a very long time.

### Precision Orbit Determination/Gravity

The traditional strength of SLR has been in the ability to determine the orbits of target satellite with high accuracy. In the case of TOPEX/POSEIDON, SLR is the primary means of precisely determining the orbit to the required 13 cm in the radial component in support of radar altimeter analyses. SLR tracking of NASA altimeter satellites has been an important element in the accomplishment of the respective mission goals. SLR, however, has a distinct disadvantage created by dependency on atmospheric transparency. Radiometric systems, such as GPS and DORIS, are potentially able to provide essentially continuous tracking. Since TOPEX/POSEIDON includes SLR, GPS and DORIS, it will provide a unique opportunity to evaluate the performance of all systems. The focus of tracking systems on future satellites may be GPS with SLR as a backup. Nevertheless, it is important to note that the passive nature of SLR provides an extremely reliable space segment--it simply will not fail except under catastrophic circumstances. A cautionary note for the future is in order. The risk of regarding SLR as a backup system encourages the reduction in operating systems for budgetary reasons, but as systems close, it becomes more difficult to reactivate them in the event that the backup mode must be initiated.

Improvements in the gravity field, including the gravitational parameter GM, are other areas where SLR has made very significant contributions. The development of new models in preparation for TOPEX/POSEIDON have benefitted from the SLR data base that has been accumulated over the years, some of which has been used in previous fields and some has not. Gravity fields used for GPS applications, such as the Department of Defense WGS-84, have used SLR data from Lageos and Starlette which have particularly contributed to determination of low degree and order gravity coefficients. Current GPS applications use GEM-T3 or other, more recent fields, which have relied on SLR data. Furthermore, the Etalon satellites can be used to study gravitational effects that will be somewhat similar to those influencing the GPS satellites, except for the particular GPS effect of deep gravitational resonance.

SLR has made unique contributions to the study of temporal variations in the gravity field, both tidal and non-tidal variations. These studies have, in part, been made possible by the nature of low area-to-mass ratio satellites (Lageos and Starlette), which diminish the nongravitational forces. This diminishment enhances the opportunity to identify the spectral content of gravitational effects. Furthermore, the study of temporal changes in gravity has been enhanced by the ability to investigate the orbit evolution over long periods of time, spanning in some cases more than 15 years.

## Earth Orientation/Reference Frame

All satellite techniques are, conceptually, able to define a reference frame coincident with the center of mass. VLBI, by using extragalactic radio sources, is insensitive to the center of mass; however, if VLBI is used to track artificial satellites, VLBI would have the sensitivity of the other satellite techniques. The SLR precision and long term continuity (Lageos was launched in 1976) has been a consideration in adopting the SLR origin to be the origin of the International Earth Rotation Service Terrestrial Reference Frame.

All space geodetic techniques have demonstrated sensitivity to polar motion. Current comparisons between polar motion series obtained from SLR and those obtained from VLBI show agreement at the 0.5 milliarcsecond level. GPS developments are underway, including the proof of concept International GPS Geodynamics Service (IGS) slated to begin in June 1992.

VLBI provides long term UT1 that cannot be matched by the satellite techniques at the present time. Lageos has been demonstrated to provide independent determinations of UT1 over a 50 day interval. The higher altitude of the Etalon satellites suggests that a much longer period of UT1 determination is possible, but the sparse SLR tracking of the Etalon satellites has allowed only limited demonstrations of the UT1 capability. It is worth emphasizing that the low area to mass ratio of Lageos and Etalon result in much smaller nongravitational forces than the GPS satellites. The nongravitational forces are a significant factor in the GPS satellites that limit the use of these satellites to very short term UT1 (sub-daily to a few days).

Comparisons have been made between SLR and VLBI reference frames using collocated instruments, either permanent or mobile. These comparisons have shown agreement at the 2 cm level.

## FUTURE

With the launch of Lageos-2, there will be two Lageos and two Etalon satellites. Within a few years, a second Starlette satellite will be launched. Starlette and Lageos have provided much of our knowledge about variations in the gravity field as well as contributing to the development of gravity models for science applications and for precision orbit determination. Two Lageos satellites, for example, will enable improved Earth rotation determination and more rapid determination of site positions. New developments in on-site software have enhanced the ability of SLR to provide high precision quick-look data that can be used for science applications and to assure tracking of the diverse constellation of satellites now available for SLR tracking. Nevertheless, only one satellite can be ranged at a time and the involvement of the science community in the process of establishing priorities is essential.

No single space geodetic technique can meet all of the application requirements of the science community. Each technique provides some unique contribution, though most of the techniques overlap in some areas. In an era of diminishing budgets, the determination of the appropriate balance of techniques and the prospects of losing or eliminating some science applications must be considered as emphasis is redistributed.

The international collaboration in the SLR community has been outstanding. The promotion of further collaboration will enhance the prospects for long term availability of a global SLR network, thereby assuring the continued collection of data for the purpose of gaining better scientific understanding of our planet.